BAKU STATE UNIVERSITY NEWS

№4 *Physics-Mathematical Sciences Series* *2013*

PHYSICS

UDC 621.382

FEATURES OF ADDITIONAL ELECTRIC FIELD IN REAL METAL - SEMICONDUCTOR CONTACTS

R.K. MAMEDOV
The Baku State University
rasimaz50@yahoo.com

This review describes the physical basis of a previously unknown physical phenomenon of occurrence of additional electric field (AEF) in the metal - semiconductor contact (MSC). The paper presents the results of the direct measurement of the AEF by Atomic Force Microscopy in the MSC with different configurations, geometric dimensions, contact materials and the distances between the contacts. Specific characteristics of AEF in the electrical, thermoelectric, photovoltaic and constructive – technological experimental measurements of the MSC with the macro, micro and nanostructures are shown.

Key words: contact metal - semiconductor, Schottky diode, Schottky barrier, additional electric field, semiconductor converters.

Previously unknown physical phenomenon of occurrence of additional electric field (AEF) in the metal - semiconductor contact (MSC), established as a result of the intensive research works in the light of the detailed reliability analysis of the theoretical and experimental comprehensive studies conducted by outstanding scientists of the known Scientific Centers in the world using the latest technologies, techniques and methods of the modern microelectronics and nanotechnology [1,6]. It is the third discovery after the discovery of two diode and transistor effects in a wonderfully simple contact metal - semiconductor.

The first discovery of the diode effect by F. Braun in 1874 [2] and the second discovery of the transistor effect by D. Bardin , U. Bratteyn and U. Shokli in 1949 [3] in the ordinary MSC are the fundamental scientific principles of scientific and technological advances in the development of the radioelectronics and transistor electronics in the first and the second half of the last century, and the authors of these discoveries won the Nobel Prize. None of the discoveries of modern physics so directly affect the people's lives , as transistor effect [4]. Undoubtedly, the new phenomenon of the AEF in the same MSC can

significantly improve the prospects of the rapid development of the modern electronics, especially, microelectronics and nanotechnology.

This review describes the physical basis of the AEF in the MSC, the results of direct measurement of the AEF with methods of atomic force microscopy (AFM) and are shown specifics of the AEF in electrophysic, thermoelectric , photovoltaic and constructive - technology experimental characteristics of the MSC .

Essence of the phenomenon of the additional electric field in the real metal - semiconductor contacts

The physical mechanism of the AEF in the MSC similar physical mechanism of the formation of a potential barrier in the MSC on idealized theoretical Schottky model [5]. According to this model, if a certain surface of the metal with a work function Φ_M is in direct contact with the surface of the semiconductor n - type with a work function Φ_S and $\Phi_M > \Phi_S$ (figure1a), the MSC has the diode properties and due to contact potential difference contacting surfaces in the contact region of the semiconductor depletion layer with a depth d_o is formed and in which a potential barrier with a height of $\Phi_B = \Phi_M - \chi$ (here χ - electron affinity of semiconductor). The potential barrier under the influence of the image force is reduced by the amount $\Delta\Phi_B$ and its maximum is located at a distance x_m from the surface of the metal. Energy diagram of the Schottky diode is schematically shown in figure1b.

In fact [6], the work function (~ 4.5 eV) of free surfaces of the metal and semiconductor adjacent contact surface remain unchanged in their direct contact and the potential barrier height of contact surface become the order of 1 eV. Occurrence the contact potential difference between the contact surface and the adjacent free surfaces of the metal and the semiconductor forms AEF with a big enough intensity around the metal contact. This is shown schematically for the MSC with wide contact surface and a sufficiently large thickness of the metal in figure1c, and a lower metal thickness in figure1d, wherein AEF covers the free metal surface and penetrates into the semiconductor to a depth d. Maximum value of the AEF in the contact region of the semiconductor, directed from the contact surface to the free surface of the metal and the semiconductor, it is comparable with a similar intensity of the Schottky diode. Therefore, the MSC is characterized by two potential barrier heights at the edge (Φ_{B1}) and central (Φ_B) contact areas and its energy diagram schematically depicted as in figure 1e.

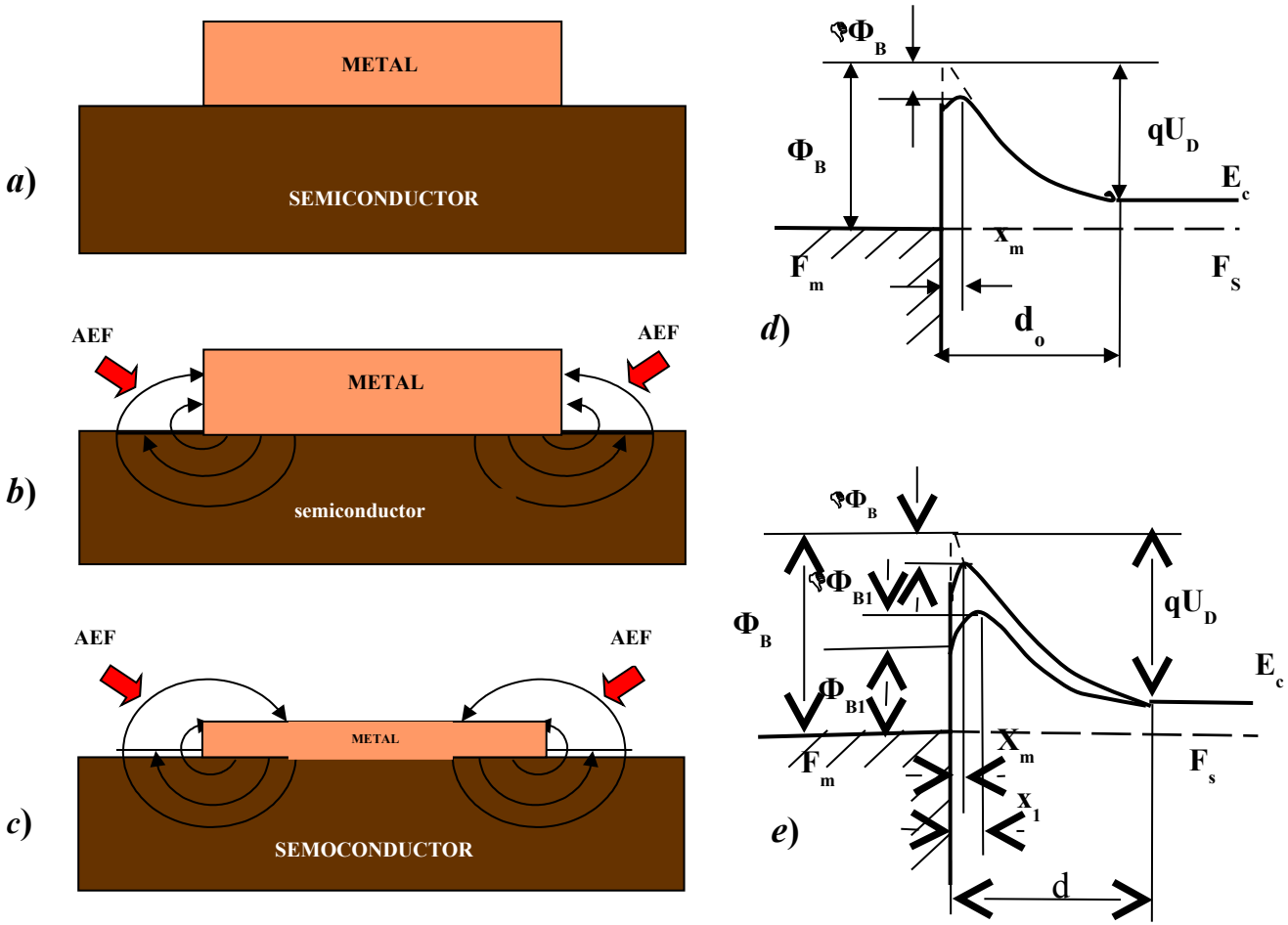

Figure 1. Schematic structures of the contact metal - semiconductor with a wide contact surface without AEF (a), with AEF and a large thickness of the metal (b), with AEF and lower metal thickness (c). Energy diagrams rectifying wide metal contact with the n-type semiconductor without AEF (d) and with the AEF (e).

For sufficiently narrow MSC with micro- and nanometer-sized contact surface the AEF penetrates the semiconductor and completely covers the contact region of the semiconductor. At the same time MSC is characterized by a single active barrier height (Φ_{BA}), formed as a result of superposition of the AEF and the field of the space charge region (SCR).

According to the basic known laws of the electrostatics, the force and the energy characteristics of AEF determined by the configuration, the geometrical dimensions of the MSC, the electrophysical parameters and nature of the contacting materials. In this context, tensions and potential the AEF of the MSC with some constructive structure, their distribution around the contact becomes dependent of the structural and technological parameters, in particular , the curvature of the side surface, the thickness of the metal, the conductivity type and the impurity concentration of the semiconductor. As the distance from the metal surface to the outer boundary of the field space AEF of MSC the tensions and potential of AEF reduced. With increasing the thickness and decreasing the curvature of the side surface of the metal of MSC expansion occurs AEF field space around the contact and, on the contrary, with decreasing the thickness, and increasing the curvature of the lateral surface of the metal is a spatial restriction AEF field space around the contact.

Moreover, the tensions of the penetrating inhomogeneous AEF into the semiconductor is directed from the contact surface of the metal to the free surfaces of the semiconductor and metal (figure 1b,c) and it participates in the formation of the potential barrier and current flow in the MSC with certain design parameters.

The results of direct measurements by AFM with high spatial resolution and accuracy of the potentials of the AEF MSC and their dependency on the geometrical parameters of contact and electrophysical parameters of the semiconductor are in good agreement with the foregoing physical properties of AEF.

AFM measurements features AEF MSC depending on the diameter and the thickness of the metal contact

AFM images of the space topography, phase contrast and contact potential difference (CPD) between the probe (W_2C) of cantilever and the surface of the epitaxial Au - nGaAs (100) Schottky diodes with different diameters 5,15, 30, 50 μm and the thickness of the metal 0.2 μm obtained in [7] shown in figure 2.

On the topography image (first column "surface") are clearly visible single round contacts. Phase contrast images (second column "phase") confirm and supplement findings relief. Phase contrast of the same surface of the GaAs contact both near the perimeter, and on the free surface away from the contacts. AFM images of the potential (the third column "potential") that measured the CPD in the contact area significantly smaller than the measured CPD on the

surface of the epitaxial n -type GaAs. Around the perimeters of contacts formed by the action of AEF axisymmetric extended region (aureole) wide *l* CPD different from CPD the free surface nGaAs ($N_D = 3.10^{15}cm^{-3}$). As the distance from the perimeter of the contact AEF tension decreases and under its influence the value of the AEF aureole on the free surface gradually increases from the minimum characteristic of CPD the metal surface ($\Delta\varphi_m$), to a maximum value ($\Delta\varphi_s$), characteristic of the free surface of CPD the nGaAs. At the same time, you can see a regular increase in the width of the aureole potential change *l* extension field space AEF with increasing contact diameter (D), i.e. with decreasing curvature the circle metal edge .

Figure 2 also shows the space h (x) and potential Δφ (x) section of surface topography on the venue dashes for nGaAs and metal contacts with a diameter of 5; 15; 30 and 50 μm. It is seen that the metal region corresponds to the region of maximum lowering the CPD and the gradual removal of the contact along the surface (on the x-axis) at a distance value *l* under the influence of the CPD of the AEF gradually increases to the free surface of the CPD of the GaAs.

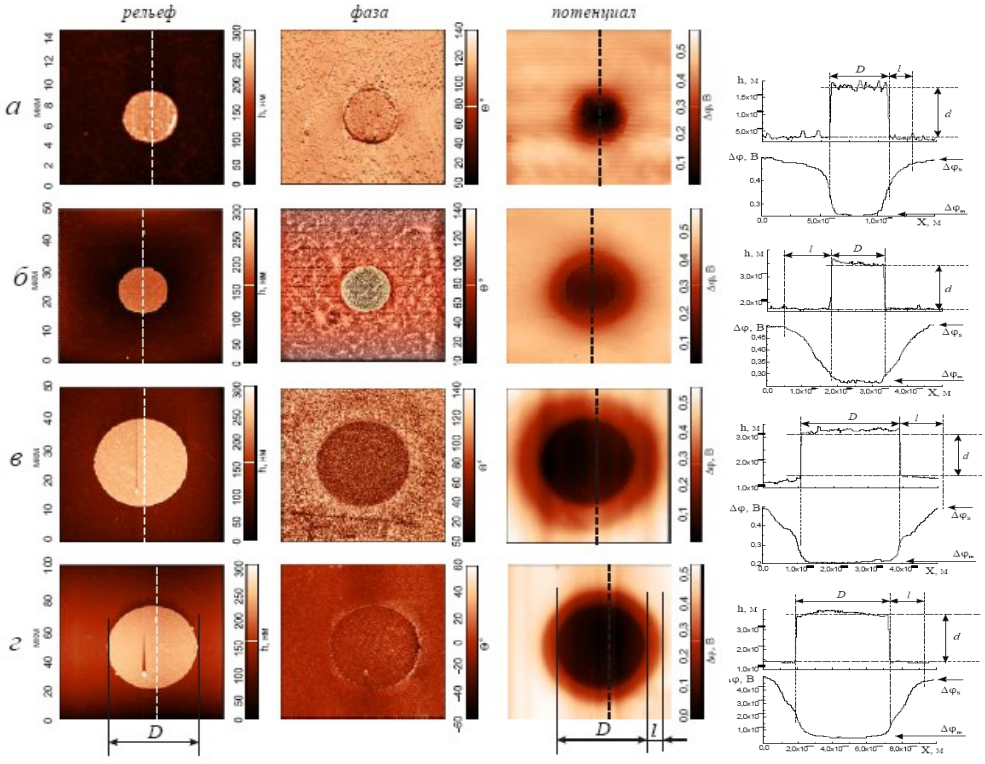

Figure 2. Two-dimensional AFM images of the topography,the phase contrast, the CPD, the space h (x) and potential Δφ (x) cross sections of the surface relief nGaAs (100) with donor concentration 3.10^{15} cm^{-3} located on it metal (Au) thickness d= 0.2 μm diameter D: a) 5 μm, b) 15 μm, c) 30 μm and d) 50 μm.

The results of the AFM measurements of CPD the contact $\Delta\varphi_m$ (where, $\Delta\varphi_m = \varphi_{W2C} - \varphi_m$) and the free surface of the semiconductor $\Delta\varphi_s$ (where, $\Delta\varphi_s = \varphi_{W2C} - \varphi_s$), potential change $\Delta\varphi$ (where, $\Delta\varphi = \Delta\varphi_s - \Delta\varphi_m$), aureole width *l* of AEF, the work function of the contact metal φ_m for epitaxial Au-nGaAs (100) Schottky diodes with different diameters D and different thicknesses of the metal d, and changing work function of the contact under the action of the AEF $\Delta\varphi_{Au-m}$ (where $\Delta\varphi_{Au-m} = \varphi_{Au - \varphi m}$) with respect to the work function of gold φ_{Au} the continuous film on the surface of n^+ GaAs are shown in Table 1.

Table 1 shows that with increasing diameter of the contacts 5 and 50 μm for the MSC to the thickness of the metal equal to about 0.2 μm is increased width *l* of aureole from 2 to 25 μm and the magnitude $\Delta\varphi_{s-m}$ from 0.230 to 0.500 eV for the MSC to metal thickness equal to about 0,075 μm *l* is increased from 1.5 to 8 μm and the magnitude $\Delta\varphi_{s-m}$ from 0.18 to 0.33 eV. At the same time, under the influence of AEF output contacts are reduced by $\Delta\varphi_{Au-m}$ relative to the work function of a continuous film on the surface of gold φ_{Au} on the n^+GaAs (where φ_{Au} = 5,124 eV) and this change becomes more significant with decreasing diameters contacts. For the MSC with a thickness of 0.2 μm metal and a diameter of 5 μm, this decrease is 0.572 eV, and for the MSC with a diameter of 50 μm - is 0.232 eV. Further AFM study shows that for epitaxial Au - nGaAs (100) in contact with a diameter greater than 100 μm influence AEF becomes non-significant.

Table 1

The numerical values of the AFM measurement method CPD of Au-nGaAs MSC structures with different diameters (5 - 50 μm).

D, μm	5	15	30	50
d = 0,2 μm , φ_{W2C}=4,902 eV, φ_{Au}=5,124 eV				
$\Delta\varphi_м$, eV	0,25	0,26	0,19	0,01
$\Delta\varphi_s$, eV	0,48	0,51	0,49	0,51
$\Delta\varphi_{s-m}$, eV	0,23	0,25	0,30	0,50
l, μm	2	13	17	25
$\varphi_м$, eV	4,652	4,642	4,712	4,892
$\Delta\varphi_{Au - м}$, eV	0,572	0,482	0,412	0,232
d = 0,075 μm, φ_{W2C}=4,902 eV, φ_{Au}=5,124 eV				
$\Delta\varphi_м$, eV	0,33	0,30	0,28	0,17
$\Delta\varphi_s$, eV	0,51	0,5	0,52	0,5
$\Delta\varphi_{s-m}$, eV	0,18	0,20	0,24	0,33
l, μm	1,5	3	7	8
$\varphi_м$, eV	4,572	4,602	4,622	4,732
$\varphi_{Au} - \varphi_м$, eV	0,552	0,522	0,502	0,392

AFM study features AEF MSC various diameters depending on the conductivity type of the semiconductor

AFM measurements of Schottky diodes with diameters of 5 , 15, 30 , 50, 100 , 200 and 500 μm fabricated from metal contact Au thickness of 0.2 μm with semiconductors as n- type and p- type epitaxial GaAs were carried out in [8]. AFM images of the space topography, phase contrast and the CPD between the probe W_2C cantilever and the surface of Schottky diodes based on n - type GaAs similar AFM images shown as in figure 2. However, for p - type GaAs, around the perimeters of the contacts formed by the action of AEF axisymmetric extended region (aureole) significantly narrow width *l* of CPD from personal - free surface of the CPD of nGaAs ($N_A = 5.10^{18}$ cm^{-3}). Figure 3 are represented the AFM images of the space topography (I), the contact potential difference (II) with corresponding cross-sectional profile (III) surface sites of the p - type GaAs, containing the gold contacts with diameters 5 (*a*), 50 (*b*) and 500 μm (c).

For Au-nGaAs and Au-pGaAs with metal thickness of 0.2 μm results AFM measurements CPD the contact $\Delta\varphi_m$ (where, $\Delta\varphi_m = \varphi_{W2C} - \varphi_m$) and the free surface of semiconductors $\Delta\varphi s$ (where, $\Delta\varphi_m = \varphi_{W2C} - \varphi_s$), potential change $\Delta\varphi$ (where, $\Delta\varphi = \Delta\varphi s - \Delta\varphi m$), aureole width *l* of AEF, the contact metal work function φ_m for epitaxial Au-nGaAs (100) Schottky diodes with different (5 - 500 μm) diameter D, as well as changes in the work function of contact under AEF action $\Delta\varphi_{Au\text{-}m}$ (where $\Delta\varphi_{Au\text{-}m} = \varphi_{Au} - \varphi_m$) relative to the work function of a continuous film on the surface of gold φ_{Au} on the n^+GaAs are shown inTable 2.

From Table 2 it can be seen that Au-nGaAs, MSC with increasing diameters from 5 to 500 μm width is increased aureole *l* of 4 to 26 μm and the magnitude $\Delta\varphi_{s\text{-}m}$ from 0.10 to 0.62 eV. At the same time, under the influence of AEF output contacts are reduced by $\Delta\varphi_{Au\text{-}m}$ relative to the work function of a continuous film on the surface of gold φ_{Au} on n^+GaAs (where φ_{Au} = 5,124 eV).

For the MSC with a diameter of 5 μm, this decrease is 0.492 eV , and for the MSC with a diameter of 500 μm - is 0.092 eV. It is noted that epitaxial Au - nGaAs contact diameter greater than 100 μm the AEF effect is markedly reduced . For Au- pGaAs observed narrow width *l* of the aureole. For the MSC with a diameter of 5 μm it has a value of 2 μm and with diameters MSC increasing from 30 to 500 μm is no increase in the width *l* of the aureole and it has a value of 4 μm. This means that, unlike the n- type GaAs, p- type GaAs free positive charge carriers under the influence of the AEF forms enriched region (aureole) around the contact with the narrow width, slightly depending on the curvature of the metal edge .

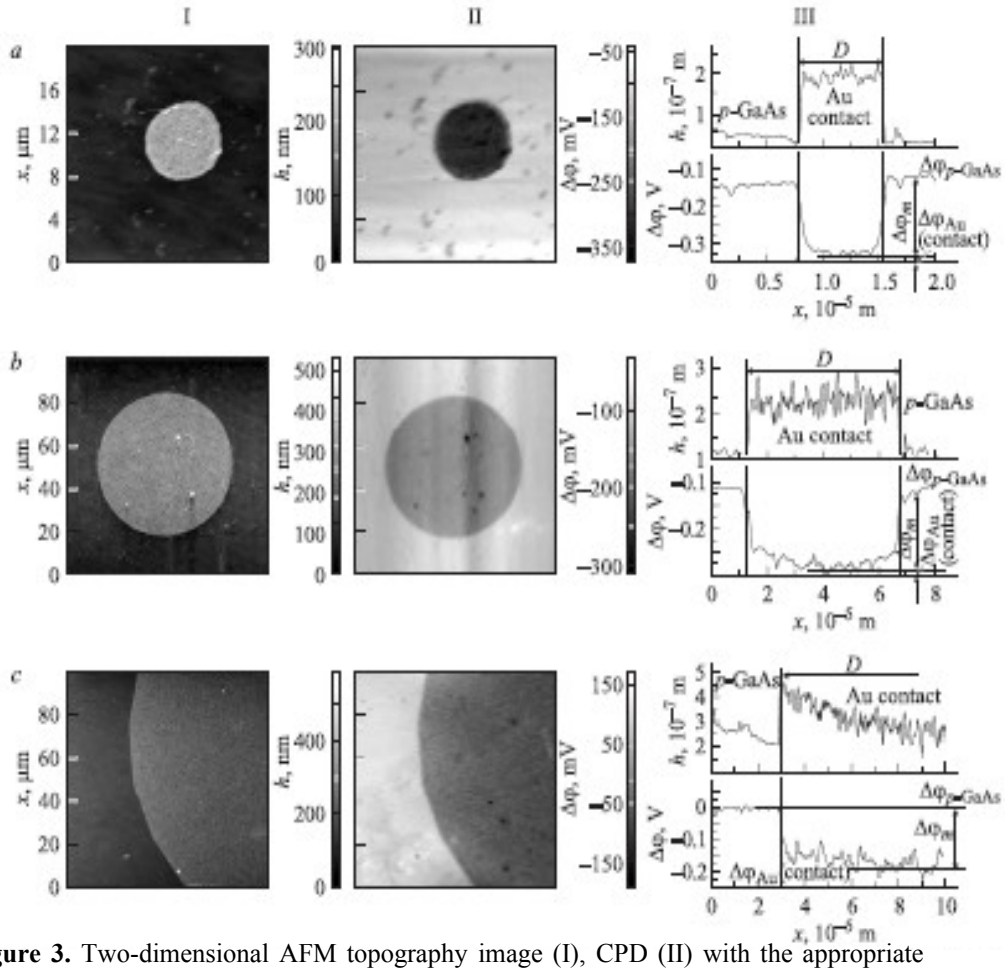

Figure 3. Two-dimensional AFM topography image (I), CPD (II) with the appropriate space h (x) and potential Δφ (x) cross sections (III) surface reliefs pGaAs (100) disposed there on metal (Au) thickness d =0.2 μm diameter D : a) 5 μm; b) 50 μm and c) 500 μm.

Table 2

The numerical values of the AFM measurement method CPD of Au-nGaAs and Au-pGaAs MSC structures with different diameters (5 - 500 μm).

D, μm	5	15	30	50	100	200	500
Au-nGaAs, d = 0,2 μm, φ_{W2C}=4,902 eV, φ_{Au}=5,124 eV							
$\Delta\varphi_м$,eV	0,270	0,230	0,170	- 0,030	- 0,070	- 0,120	- 0,130
$\Delta\varphi_s$, eV	0,370	0,375	0,430	0,420	0,490	0,480	0,490
$\Delta\varphi_{s\text{-}m}$, eV	0,100	0,145	0,260	0,450	0,560	0,600	0,620
l, μm	4	12	16	20	23	24	26
$\varphi_м$, eV	4,632	4,672	4,732	4,932	4,972	5,022	5,032

φ_{Au} -$\varphi_м$, eV	0,492	0,452	0,392	0,192	0,152	0,102	0,092
Au-pGaAs, d = 0,2 μm, φ_{W2C}=4,902 eV φ_{Au}= 5.323 eV							
$\Delta\varphi_м$, eV	- 0,322	- 0,320	- 0,290	- 0,280	- 0,180	- 0,090	- 0,180
$\Delta\varphi_s$, eV	- 0,126	- 0,150	- 0,130	- 0,130	- 0,040	0,040	0,000
$\Delta\varphi_{s\text{-}m}$, eV	0,196	0,170	0,160	0,150	0,140	0,130	0,180
l, μm	2	3	3.5	4	4	4	4
$\varphi_м$, eV	5,224	5,222	5,192	5,182	5,082	4,992	5,082
φ_{Au} -$\varphi_м$, eV	0,099	0,101	0,131	0,141	0,241	0,102	0,241

AFM study of features AEF MSC depending on the geometrical configuration of the contact.

The results of the AFM measurements of the epitaxial surface nGaAs with rectangular gold contacts (100x300 μm ^{2}) thickness 0.17 μm [9] are shown in figure 4. Aureole AEF width in this case is 30 μm along the straight edges of the metal due to a large contact area. As noted in this paper , the effect of AEF on the MSC potential outside is so great that the presence of a nearby metal contact at a distance of 200 μm capacity does not exceed the level corresponding to the free surface. It should be noted that the aureole around the corner rounding contact is much narrower than in the rest area. This is consistent with the width of the aureole decreases with decreasing diameter of the contact, i.e. AEF field space width with increasing curvature of the peripheral surface of the contact, as mentioned above.

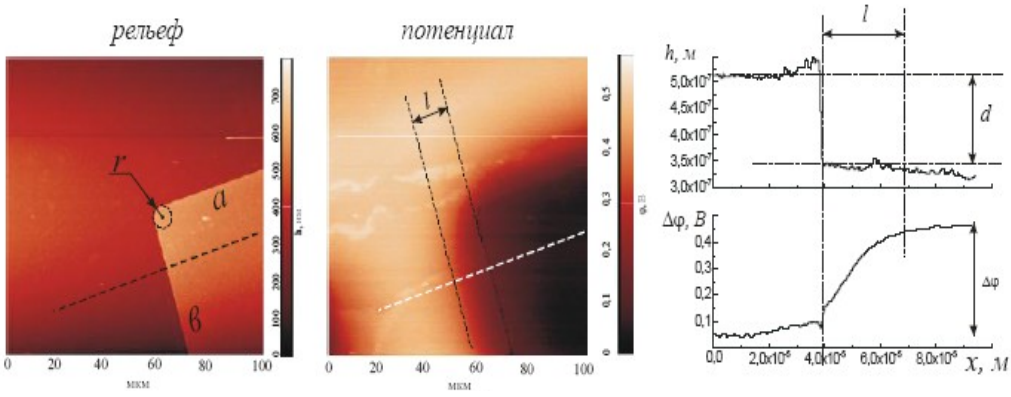

Figure 4. Two-dimensional AFM topographic image (column "relief"), CPD (column "potential") of the surface of epitaxial nGaAs (100) with a charge carrier concentration N_D = 3 • 10^{15} cm^{-3} placed on it a rectangular 100x300 μm^2 Au-contact thickness 0.17 μm, and the relevant sections of the longitudinal profiles of the space h (x) and the potential Δφ (x) the reliefs on the dotted lines.

AFM study of the distribution of potential AEF MSC at the free surfaces of the semiconductor and the contact metal

To determine the patterns of distribution of potential AEF on MSC with AFM method was used cross-sectional profiles CPD epitaxial Au - nGaAs (100) in contact with a diameter of 200 μm and a metal thickness of 0.150 μm[10] , which are presented in figure 5. The figure shows that the distribution of the potential for AEF with aureole width of about 25 μm (figure 5a), on the periphery of the contact at a distance of about 2 μm (figure 5 b) , and the contact surface at a distance of about 50 μm (figure 5c) considerably differ from each other. It can be seen that the value of CPD to the free surface of the semiconductor in the contact edge of the aureole decreases linearly. The length of the linear portion of the CPD profile is 22.5 μm. In this part of the value of the surface potential is changed by 90 mV. On the metal surface from the edge to the center of the contact at a distance of about 50 μm CPD value decreases almost exponentially. Between these portions of the change in the CPD on the contact periphery width of about 2 μm is given, as shown in figure 5b.

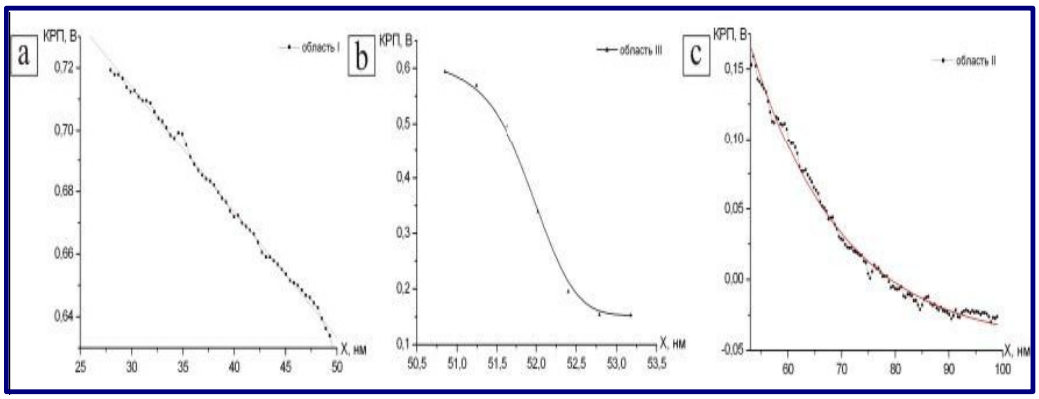

Figure 5. Cross-sectional profiles CPD epitaxial Au -pGaAs (100) in contact with a diameter of 200 μm and 0.150 μm thick metal :aureole with about 25 μm wide (a), the periphery of the contact at a distance of about 2 μm (b) and the contact surface at a distance about 50 μm (c).

AFM study of the interactions of AEF MSC depending on the distances between the contacts

Figure 6 shows AFM images of Au - nGaAs (100) the MSC with a diameter of 10 μm and a metal thickness of 0.06 μm at different multiplicities of the distances between them [10]. It is seen that for a single distance in the contact area there is a general decrease in the magnitude of CPD on the semiconductor surface. When the distance between the contacts on the measured

surface potential on the surface nGaAs increases and tends to the value, the corresponding free surface.

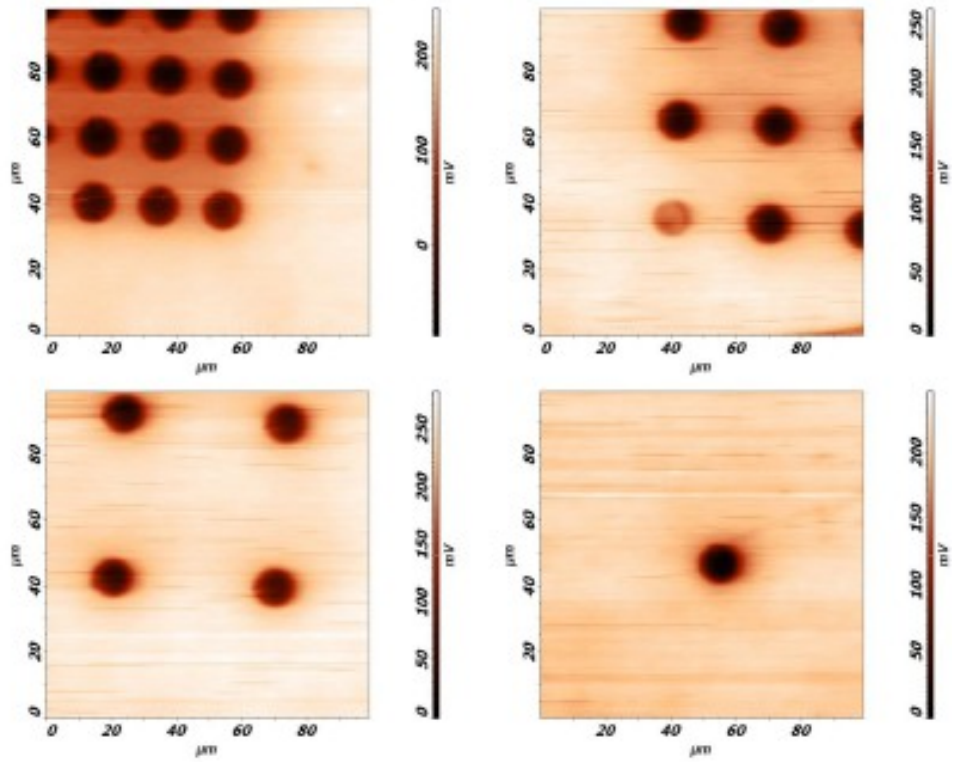

Figure 6. AFM images of an epitaxial Au - nGaAs (100) contacts with a diameter of 10 μm and 0.060 μm thick metal at different multiplicities distances there between.

Figure 7 shows AFM images of the two plots 100x100 μm^2 of the surface epitaxial nGaAs, containing single Au contacts with diameter of 10 μm and the matrix quadruple (40 μm) and single (10 μm) distance between the contacts [11]. The relief images (a) and CPD (b) with the corresponding profiles (c), space h (x) and potential $\Delta\varphi$ (x) cross-sectional the surfaces shows that reducing the distance between the contacts leads to a marked decrease in CPD (higher potentials) on the contact surfaces and the surface of the epitaxial nGaAs in intervals between contacts . Further reduction in the distance between the contacts to 10 μm lowers the CPD unit contacts and the semiconductor surface.

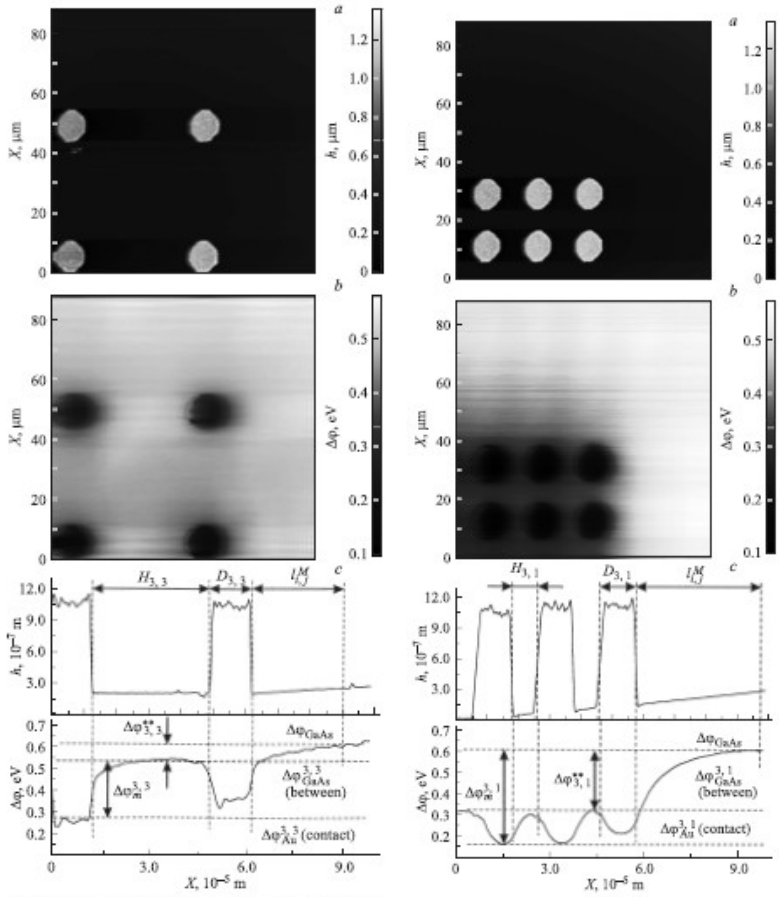

Figure 7. AFM images of two sections of 100x100 μm^2 surface of the epitaxial nGaAs, containing single Au contacts with diameter 10 μm matrix quadruple (40 μm) and single (10 μm) distance between the contacts: (a) the topography and (b) the CPD with the corresponding profiles (c) space h (x) and potential Δφ (x) cross-sections of the surfaces.

AFM study of features AEF MSC depending on the nature and thickness of metal

To study the features of AEF depending on the nature and thickness of the metal by AFM measurements carried out in the MSC [7] on the basis of contact platinum (Pt) with a thickness of 0.2 μm and 0.1 μm and with semiconductor nGaAs with concentration donor impurity $N_D = 6.10^{16}$ cm^{-3}. Two-dimensional AFM topography image (column " relief"), phase (column " phase") and CPD (column "potential") surface nGaAs (100) located on it the diode matrix formed metal platinum with a diameter of 5 μm (a) and 0.1 μm (b) with the corresponding space profiles of longitudinal sections h (x) and the potential Δφ (x) reliefs on the dotted lines are presented in figure 8 . It can be seen that the relative behavior of the quantities $\Delta\varphi_m$, $\Delta\varphi_s$ and $\Delta\varphi_{s\text{-}m}$ depending on the diamet-

er and thickness of the metal, in general, similar to the nature of the behavior of these same quantities for Au - contact. In this case the absolute values of the aureole width l and $\Delta\varphi_{s\text{-}m}$ for platinum Pt - contacts significantly higher than those values for Au - contacts of the same size. AFM images of the topography and surface potential with its cross-sectional profile of the diode array is clearly seen that for Pt - potential contact AEF to aureole also has the properties of additively. The result of adding the action potential at each point of the surface containing barrier contacts increases. This leads to a strong decrease in CPD on contact surfaces and the significantly increase the width of the aureole AEF around the diode matrix (figure 8c).

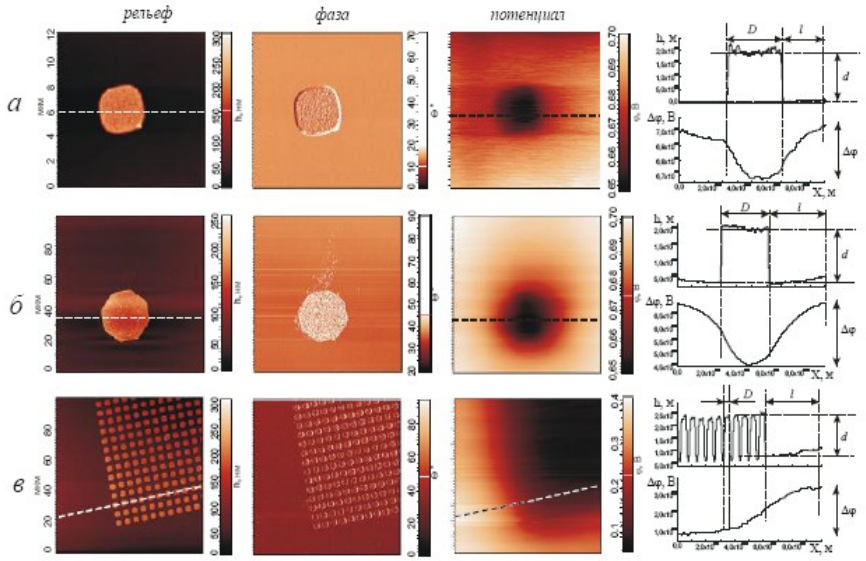

Figure 8. Two-dimensional AFM topographic image (column "relief") phase (column "phase") and CPD (column "potential") of the surface nGaAs (100) with a charge carrier concentration $N_D = 6 \cdot 10^{16}$ cm^{-3} placed in it with a diode matrix (c) the formed metal platinum (Pt) with a diameter of 5 μm and thicknesses of 0.2 μm (a) and 0.1 μm (b) with the respective longitudinal sections of the spatial profiles of h (x) and the potential Δφ (x) reliefs.

The study by scanning electron microscopy features of current transport in the MSC diodes with AEF

In an earlier paper [12] with a scanning electron microscope and electron beam induced current (EBIC) were studied especially premature breakdown in SD with a planar structure and a mesa structure. SD was manufactured applying Pt metal film on the surface the semiconductor GaAs with a donor concentration of 6.10^{15} cm^{-3} and heat - processed to 350 ° C for a time of from 1.5 to 216 hours. The energy of the electron beam was varied in the range 5-30 keV. Results of the study SD with planar and mesa structure were almost identical.

Typical images of the density distribution of the current along the contact surface of the planar Schottky diodes in the reverse bias -1; -5 and -15 V are shown in figure 9.

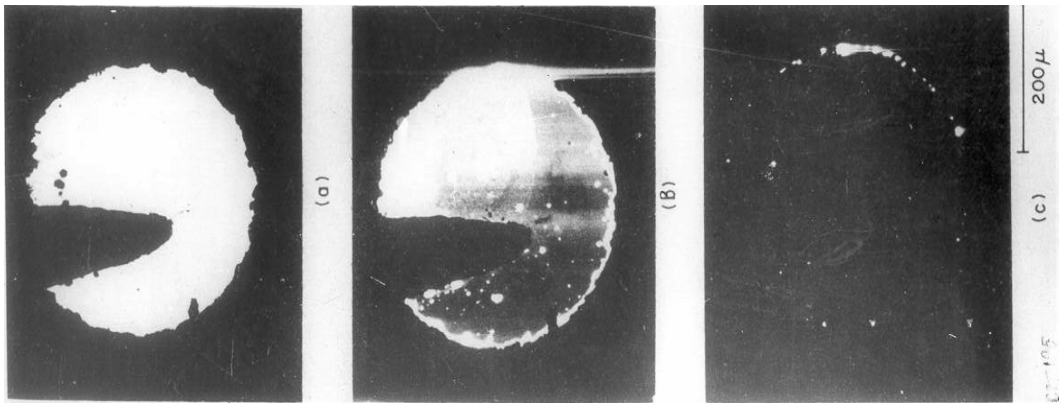

Figure 9. Current density distribution along the contact surface of Pt - nGaAs Schottky diode in reverse bias (U < 0): a) -1V, b) – 5V and c) -15V.

As seen from figure 9 and, when -1V voltage , the reverse current density is approximately evenly distributed over the contact surface and at the same time, there are some areas, through which currents hardly occur. This means that in these points AEF spots still offset from the external field [6]. At a relatively high voltage -5 V (figure 9b) there is a plurality of separate lighted areas and along the periphery of the contact luminous ring through which currents flow with high density. This shows that while AEF contact once fully compensated by the external voltage and current flow begins in the dark areas. When the reverse voltage -15 V (figure 9c) separate areas with high current density, i.e. luminous areas on the background of the lower contact mainly observed at the periphery of the contact. When this has no influence AEF. When superimposed figure 9a,b and c each other, it is found that the white portions in figure 9, with the same with the white areas in figure 10, in the distributed along the surface, including the periphery of the contact. A separate white areas and uneven white ring around the contact in figure 9, in the same areas with separate black and black peripheral region in figure 9a. This is well demonstrated experimentally as AEF in current flow in Schottky diodes .

Under the influence of heat treatment allocation contact areas through which currents flow premature breakdown significantly changed. Some of them disappear and some appear again. This distribution pattern of local areas premature breakdown Schottky diodes varies from sample to sample. This means that it alters the degree of heterogeneity of the interface, and consequently influence the degree of AEF MSC.

AFM research of features of current transport in the MSC diodes with AEF

Effect of AEF on the nature of current flow in the MSC studied by the AFM methods in [13]. In this measured current flow in the forward and reverse direction in epitaxial Au - nGaAs MSC diodes with a diameter of 15 microns (figure 10a). The resulting two-dimensional AFM images of the distribution of contrasting currents spreading contact with voltage from - 10 to +10 V with the corresponding cross-sectional profiles are presented in figure 10.

From figure 10 it is evident that in the reverse direction where the intensity of the external field and the AEF in the contact area becomes opposite MSC [6], in the peripheral region of the contact begins to pass current when a voltage - 3B, it is observed as a further figure 9b. At the same time in the MSC the AEF compensated by the external voltage.

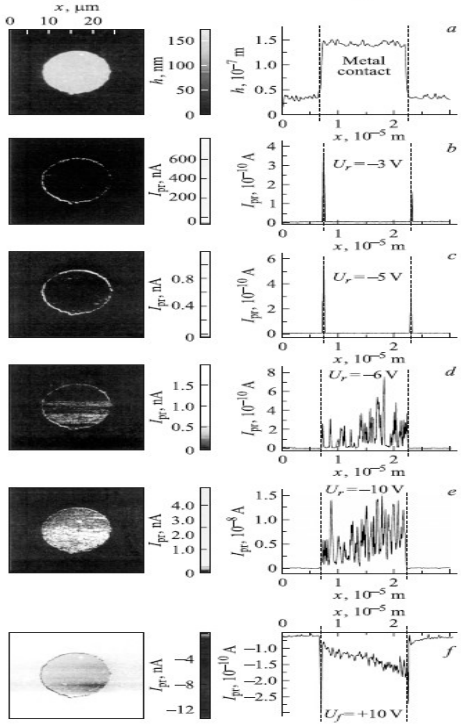

Figure 10 Two-dimensional AFM topography image and the current spreading to their profiles, cross sections of the contact Au - nGaAs Schottky diode with a diameter of 15 μm and a thickness of 0.1 μm metal.

According to figure 10b, with increasing the reverse voltage to - 5V amplitude peripheral currents is growing. This is indicated by the increasing brightness of the peripheral region of the image contrast and increases the amplitude of currents spreading peripheral area on the transverse profiles (figure 10 b,c) . The width of the peripheral region of a highly matter < 0.3 microns and practically does not vary with the applied voltage. When the inverse voltages > 6V currents through the main area becomes visible (figure 10d, e). With increasing reverse voltage amplitude the currents spreading through locally

conductive portions main contact area increases and becomes equal to the amplitude currents spreading along the periphery of the contact (or even exceed it) . The degree of localization of such sites on average 100-200 nm and is commensurate with the size of the grains forming the structure of the gold contact. When reverse voltages > 6V the AEF fully compensated by the external fields and the entire contact surface becomes conductive and further increase the reverse voltage leads to a simultaneous increase in current spreading as on the periphery, and in the main area of contact .

In forward voltage the intensity of AEF and the external field becomes parallel in the contact region and therefore, the distribution of current spreading, depending on the applied voltage changes its character [6] and becomes the way it is presented on figure 10f. Increased forward voltage does not lead to a relative change of peripheral currents.

Features of current flow in the MSC diodes with AEF depending on the contact diameter and temperature

From the above it follows that the degree of influence of both the AEF surface potentials MSC and the electronic processes in the contact region of the semiconductor (i.e. instrument characteristics of MSC) is determined by the configuration of contact and its geometric dimensions. As shown by AFM measurements AEF MSC (figure 2 - figure 8) , real MSC depending on the degree of influence of AEF is divided into two groups. The first group includes the MSC with a wide contact surface linear geometric dimensions more ~ 100 μm, where AEF basically covers the edge of the contact area. And to the second group includes the MSC with a narrow contact surface linear geometric dimensions less than ~ 100 μm, where AEF covers both full free surface metal contact and full contact region of the semiconductor.

The work [14] studied the electrophysical processes in identical Cr -nSi Schottky diodes, differing only by the geometrical dimensions, i.e. extent to AEF. The SD structure based on a contact with a chromium and the silicon n- type manufactured by standard photolithography. On planar surface with crystallographic orientation (111) of silicon wafer with a resistivity of 1 Ohm cm grown thin dielectric layer SiO_2 with a thickness of about 0.3 μm. In the SiO_2 layer were opened windows of different diameters (6 , 10, 20, 60 , 100, 200, 500 and 1000 μm) . Chromium film with a thickness of 0.5 μm were obtained by thermal evaporation under vacuum of 10^{-4} Pa on the surface of the windows SiO_2. With the aid of special methods developed in [6] were identified peripheral currents I_{LS}, flowing through the peripheral portion of the contact surface and the currents I_S, flowing through the contact surface without AEF SD. At the same time were used averaged linear density j_L peripheral currents I_L, due to only the influence of AEF SD.

Typical forward I-V characteristics of Cr-nSi SD with diameters of 10 microns, 100 μm and 1000 μm, where the intensity of the external field and the AEF in near contact region become parallel [6] , are shown in figure 11 , curves 1 , 4 and 7 , respectively. It can be seen that the experimentally observed the forward I-V characteristics

SD describes thermionic emission theory . The same figure also shows the dependence of both I_{LS} from U (curves 2 , 5 and 8, respectively) , and I_S from U (curves 3 , 6 and 9 respectively) for SD with diameters of 10 microns, 100 microns and 1000 microns. It is seen that depending how I_S, and I_{LS} from U determined by the mechanism of thermionic emission . The dependence of I_S from U in semi-logarithmic scale is linear and the dependence I_{LS} from U is nonlinear . It is found that the contact area on the periphery with the h_L and S_L of SD the barrier height Φ_{LS} becomes lower the barrier height for the rest of its Φ_{BS} contact area. Current I_F, flowing through a common contact surface SD is the sum of currents I_{FL} and I_{FS}, flowing through the peripheral area S_L and the rest of the contact area S_S-S_L.

Typical reverse I-V characteristics of Cr-nSi SD with diameters of 10 μm, 100 μm and 1000 μm, where the intensity of the external field and the AEF in near contact region are opposing [6] , are presented in figure 12 (curves 1 , 4 and 7 , respectively) in a semi-logarithmic scale. It is seen that I-V characteristics are represented by two specific participants: the first section covers the initial interval of the voltage U from 0 to about 2 , and the subsequent second section covers the range of the voltage U= 2 V to the breakdown voltage .

Current I_{R1} of first section of the I-V characteristics back slowly increases with increasing U, and this dependence decreases with increasing the diameter of the contact. Between I_{R1} and U is not observed in a correlation . However, between the current I_{R2} of second portion of the I-V characteristics and U there exists a definite correlation, i.e. with increasing U the current I_{R2} exponentially increases. When extrapolating the straight lines to the ordinate axis in figure 12 for SD with different diameters becomes clear that the current I_2 begins to flow through the contact only after applying a voltage by an amount of about 2 well as it did in figure 9 and figure 10 .

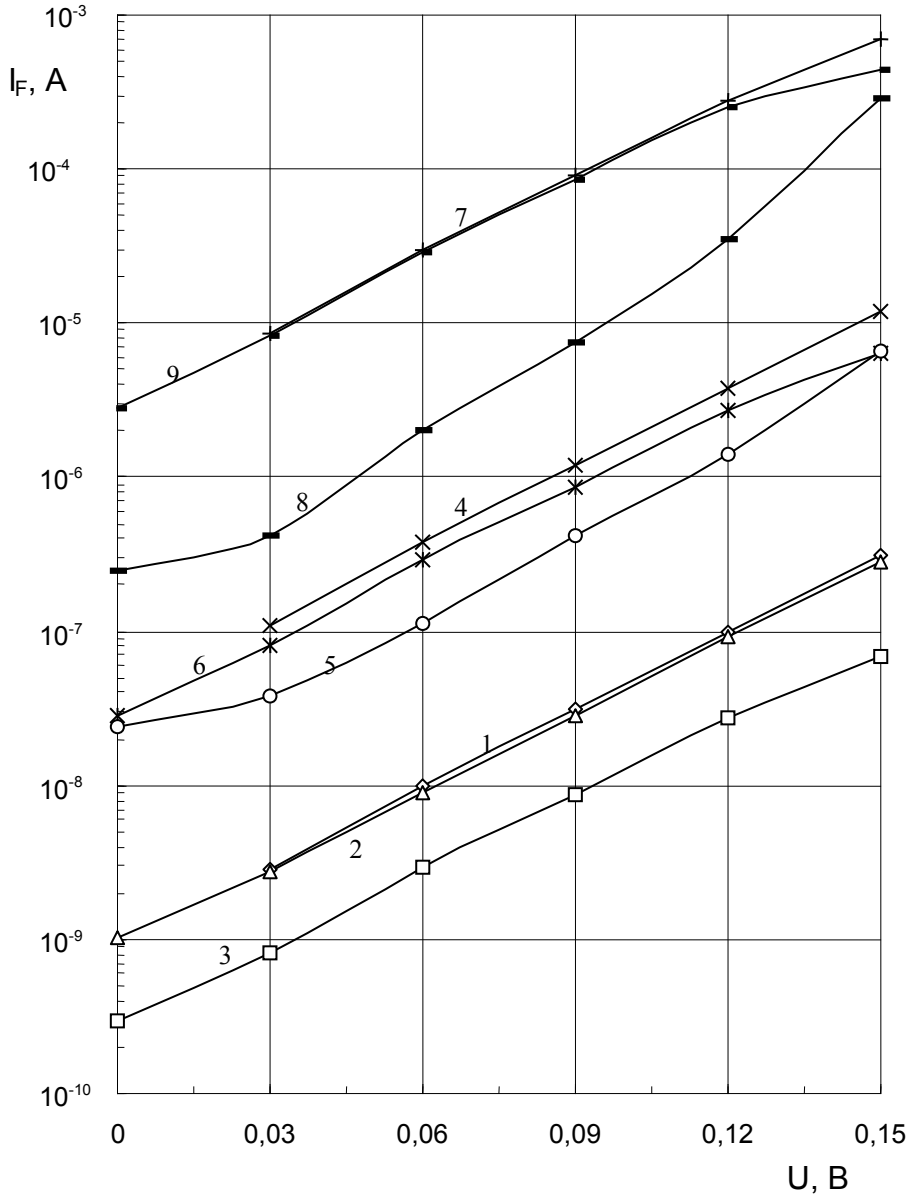

Figure 11. Forward I-V characteristics Cr - nSi Schottky diodes with diameter of 10 μm, 100 μm and 1000 μm: total contact currents I_F (curves 1, 4 and 7, respectively), peripheral current I_{LS} (curves 2, 5 and 8, respectively) total currents contact without affecting the peripheral effects I_S (curves 3, 6 and 9, respectively).

Depending I_{LS1} of the U for SD with diameters of 10 μm, 100 μm and 1000 μm are presented in figure 13 (curves 2, 5 and 8, respectively). The same figure also shows the dependence I_{S1} of the U (curves 3, 6 and 9, respectively).

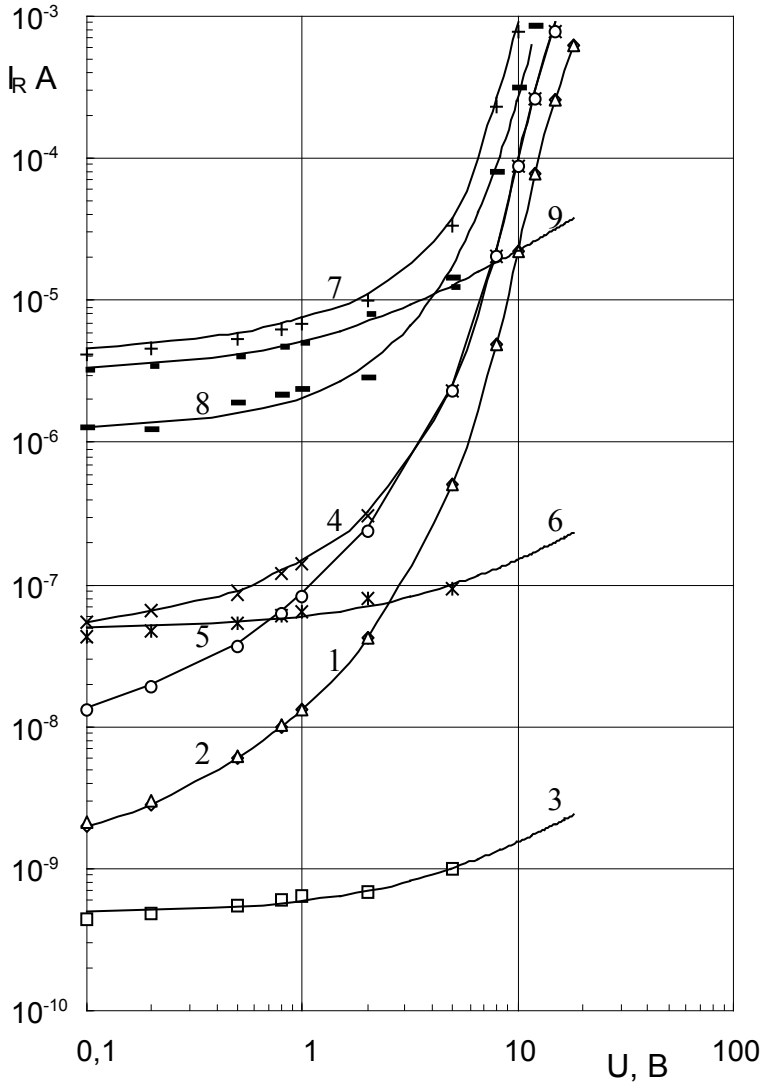

Figure 12. Reverse I-V characteristics Cr - nSi Schottky diode with diameter of 10 μm, 100 μm and 1000 μm: total contact currents I_F (curves 1,4 and 7, respectively), peripheral current I_{LS} (curves 2,5 and 8, respectively), the total current contact without affecting the peripheral effects I_S (curves 3, 6 and 9, respectively).

It is seen that depending how I_{S1} and I_{LS1} from U defined mechanisms of thermionic emission. The dependence I_S of U in semi-logarithmic scale is linear, and the dependence I_{LS} of U is nonlinear. Using the values of I_{LS1} and I_{S1} at U = 0,1 V, the I-V characteristics were identified by the potential barrier height Φ_{LS1}, dimensionless coefficient n_{L1} (at U = 1 V) SD with different diameter for the peripheral portion and total contact surface without influence AEF (Φ_{B-}

$_{S1}$, n_{S1}, respectively). From figure 12 (curves 1, 4 and 7) that the second portion of the I-V characteristics SD consists primarily of current flowing through the contact periphery and semi-logarithmic scale is a straight line. Extrapolating the straight line to the ordinate axis in figure 12 were determined saturation currents I_{L2} (0) SD with different diameters .

Thus, the experimental study of current transport in Cr-nSi SD with AEF showed:

- The total contact surface SD with AEF consists of two region (the peripheral with a width of a few micrometers and with respect to internal), in which the potential barrier height differs about 40 meV and decreasing contact diameter of 1000 μm to 6 μm contribution peripheral current to total exposure increases to about 100 % for the forward and the initial reverse I-V characteristics ;
- The potential barrier height, ideality factor (dimensionless coefficient), contact resistance and the width of the peripheral area of the contact surface, the contribution of the peripheral current to total for forward and initial reverse I-V characteristics SD with AEF have corresponding similar values ;
- For the first initial part of the I-V characteristics SD with AEF should be her second section, which is shown after the application of definitions of critical voltage and consists only of peripheral current for which the potential barrier height, the dimensionless coefficient, contact resistance and the width of the peripheral area contact surface differ from those first initial portion of the I-V characteristics;

The I-V characteristics SD with AEF in general described by a formula obtained on the basis of thermionic emission theory based on AEF [6].

In work [15] presented results of a study of the temperature dependence of the total current flowing in the Ni-nSi SD with different diameters (10 - 1000 μm) , and the results of the study of the temperature dependences of the current flow in the absence of the influence of AEF and the peripheral current these structures are presented in the following SD papers [16-18], and the concentration dependence of current transport in the paper [19].

Study [15] of the temperature dependence in the range of 132 - 387 K Ni-nSi SD with varying degrees of influence AEF showed that a satisfactory form I-V characteristics SD with AEF is stored in a limited temperature range . Features of the temperature dependence of the barrier height, ideality factor, contact resistance, dimensionless coefficient and other parameters SD with AEF depend on the temperature interval and on the geometry of the contact, i.e. the degree of influence of AEF .

From the forward and the initial portions of the reverse branches I-V characteristics SD with different diameters were determined barrier heights Φ_{BF} and Φ_{BR} in a wide range of temperatures. Their temperature dependences for SD with diameters of 10 μm, 100 μm and 1000 μm are presented in figure 14a and 14b. As can be seen from the figures, the temperature dependence of the barrier height depends both on the geometric dimensions of rectifying contact

SD, i.e. the degree of influence of AEF, and from the values of the selected temperature range. For SD with diameter of 10 μm, i.e. with a large degree of influence of AEF, the barrier height with increasing temperature in the range of 222 -311 K increases, and in the range of 311 -387 K decreases. For SD with diameter of 1000 μm, i.e. with less influence of AEF , the barrier height with increasing temperature in the range of 247 - 329 K, remains almost unchanged, but the range of 329 K to 387 K , decreases slowly . For SD with diameters greater than 10 μm and about 1000 μm depending on the temperature of the barrier height between the intermediate states are characterized by the temperature dependency of the barrier height for SD with diameters of 10 μm and 1000 μm, as represented in figures for SD with a diameter of 100 μm. Change in the sign of the thermal coefficient of the barrier height with increasing temperature, confirmed the values of barrier heights SD, certain dependencies of Richardson I_O/T^2 of 1 / T.

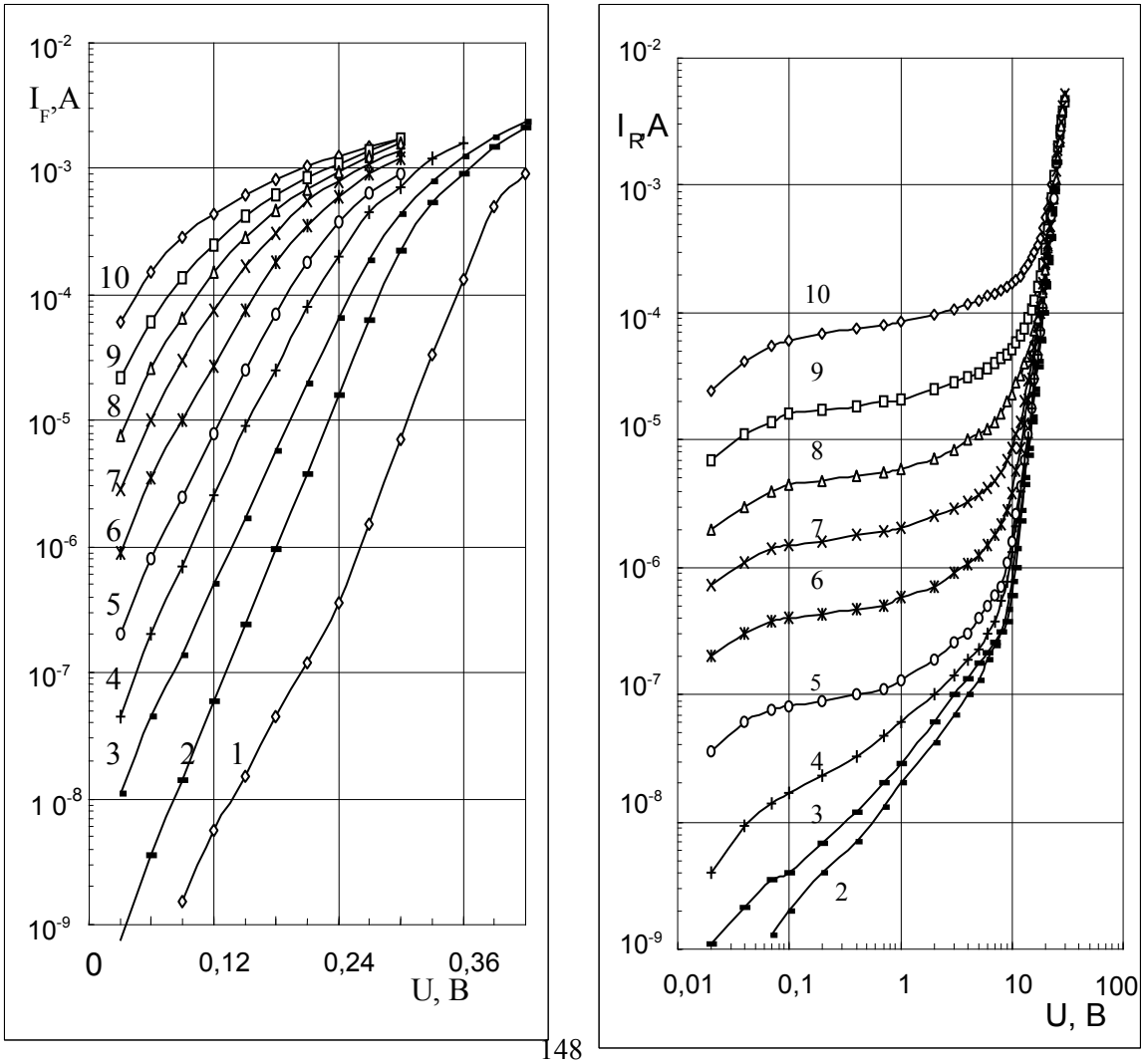

148

a) *b*)

Figure 13. Forward (a) and reverse (b) I-V characteristics Ni - nSi Schottky diode with a diameter of 100 μm at a temperature T (K): 1 – 185, 2 – 222, 3 – 247, 4 – 267, 5 – 292, 6 - 311 , 7 - 329 , 8 – 345, 9 – 363, 10 - 387.

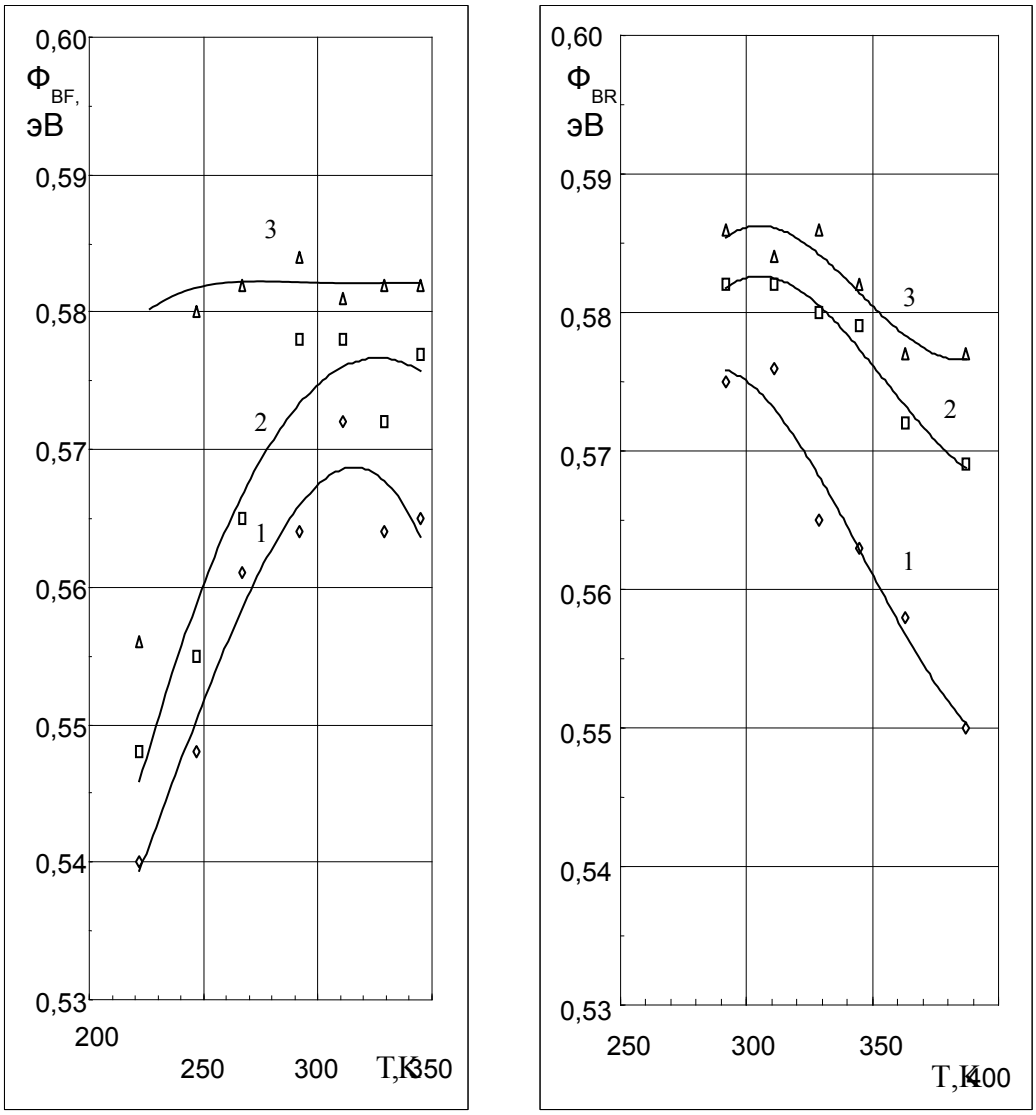

Figure 14. The temperature dependence of the potential barrier height Ni - nSi Schottky diodes with a diameter of 10 μm (1), 100 μm (2) and 1000 μm (3) for the forward (a) and reverse (b) I-V characteristics.

Thus, it should be noted that a satisfactory form I-V characteristics SD with AEF is stored in a limited temperature range, where the upper limit of the range is limited by the curvature of the I-V characteristics line in semi-logarithmic scale , and the lower limit of the interval is limited to the appearance of excess current at low voltages .

The temperature dependence of the barrier height and ideality factor SD depends on the temperature range and the degree of influence of AEF, i.e. the geometric dimensions of contact. Thus, depending on the direction of change of the temperature and the barrier height becomes opposite ideality factor, i.e. low value of the barrier height corresponds to a high value of ideality factor and vice versa. However , the exponential nature of the dependence of the contact resistance with the AEF SD temperature is maintained across the range of temperatures where the I-V characteristics SD with AEF has a satisfactory appearance. Between the experimental value of the constant Richardson and thermal coefficient of the barrier height SD with AEF exists exponential dependence. With increasing voltage the reverse current increase in SD with AEF occurs more than would be expected from the reduction of the barrier height under the influence of the image force .

The experimental results are well interpreted theories thermionic emission based on AEF [6].

Features of current transport in electrically interacted Schottky diodes with different diameters and AEF

Electrical interaction of Schottky diodes with AEF studied in detail AFM methods in [11]. When this was made SD matrix given the necessary condition of the electrical interaction between the contacts is the presence around them extending to large enough distances (<30 μm) aureole AEF . It is investigated the matrix Mi, j with gold 0.9 μm thick contact with *i* diameters ($D_{i,j}$ = 3 , 5, 10, 15 and 30 μm), and with distances between the contacts *j* ($H_{j,j}$ = 1x$D_{i,1}$ 2x$D_{i,2}$, 4x$D_{i,3}$, 10x$D_{i,4}$) formed on the surface of the epitaxial layer nGaAs (100) with a thickness of 0.3 μm and a concentration $N_D = 4.5.10^{16}$ cm^{-3} , as shown in figure 15.

Figure 16 presents the forward and reverse I-V characteristics in semi-logarithmic scale electrically SD interacting with different diameters ($D_{i,4}$ = 3 , 5, 10 , 15 and 30 microns) diode arrays $M_{i,4}$ with a tenfold by the distance $H_{i,4}$ = 10x$D_{i,4}$ between the terminals. It is found that with increasing diameter of the contacts increases the active potential barrier height and insignificantly reduced ideality factor. Current interval changes the straight lines with decreasing diameter contacts from 30 μm to 3 μm for forward bias 0.5 V was 2 orders of magnitude, from 10^{-5} to 10^{-7} A. SD breakdown voltage in the reverse current of 10 μA increases from 13 to 14.5 V with decreasing contact diameter.

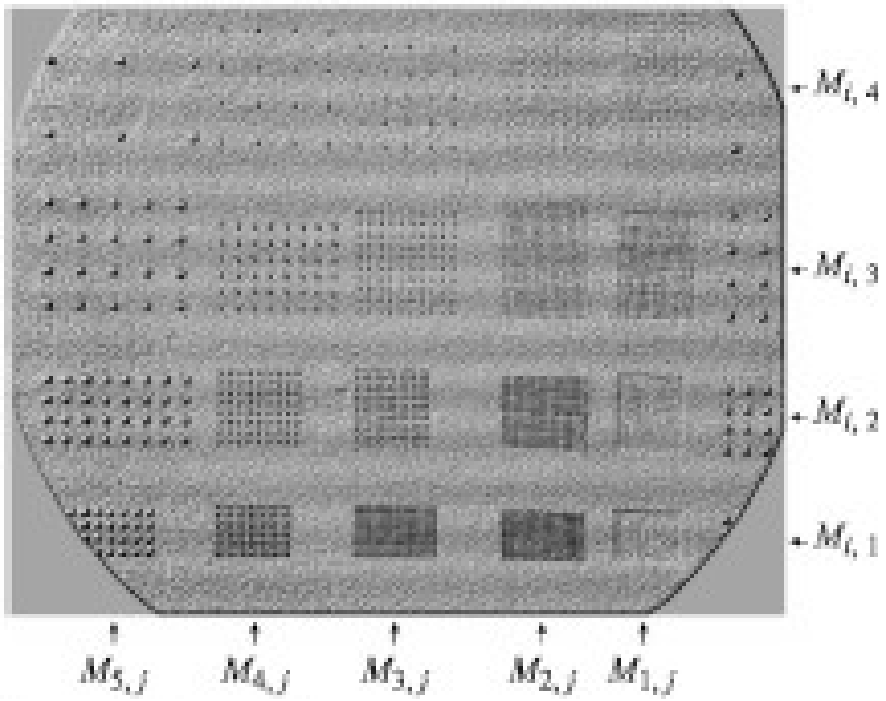

Figure 15. Photo epitaxial surface of the chip with nGaAs disposed there on matrices Mi, j (where, Di, j - the diameter of the contacts, Hi, j - the distance between contacts) gold contact DS. Integer "i" diameter contact numbers: 1 – $D_{1,j}$ – 3, 2 – $D_{2,j}$ – 5, 3 – $D_{3,j}$ – 10, 4 – $D_{4,j}$ –15 and 5 – $D_{5,j}$ – 30 μm . The integer "j" labels the distance between the contacts:1 – $H_{i,1}$=1x$D_{i,1}$, 2 – $H_{i,2}$=2x$D_{i,2}$, 3 – $H_{i,3}$=4x$D_{i,3}$ и 4 – $H_{i,4}$=10x$D_{i,4}$.

Figure 17 presents the forward and reverse I-V characteristics in semi-logarithmic scale electrically SD interacting with different diameters ($D_{i,1}$ = 3 , 5, 10 , 15 and 30 μm) diode arrays $M_{i,1}$ single by the distance $H_{i,1}$ = 1xD_i, one between the terminals. Found that the seal diode arrays of all kinds leads to significant changes in their I-V characteristics . In this case, I-V characteristics SD diameters of 3, 5 , 15 and 30 μm are close to I-V characteristics SD with a diameter of 10 μm. Variation in the forward current at 0.5 V was only 5.10^{-6} A. Thus for SD with diameters less than 10 μm, a decrease the active barrier height. For SD with diameters greater than 10 um , on the contrary , an increase in the active barrier height. Quantitative differences in qualitative agreement is also observed for the reverse I-V characteristics SD packed matrices.

Found that electrical interference between collected in diode array contacts SD appears in a significant change in their surface potential and the static I-V characteristics. Shown that the variation of the surface potential and the static I-V characteristics under the influence of SD occurs own AEF contact and under the influence of AEF matrix formed by the superposition of its constituent AEF contacts. Of such influence is determined by the distance between the contacts , as well as complete a total

charge of the space charge region of the matrix of all contacts . It was found that the convergence of contacts leads to an increase in the active barrier height and the slight increase in the ideality factor. Increase in the total contact area in the matrix leads to a relative decrease of the active barrier height and a slight increase in the ideality factor.

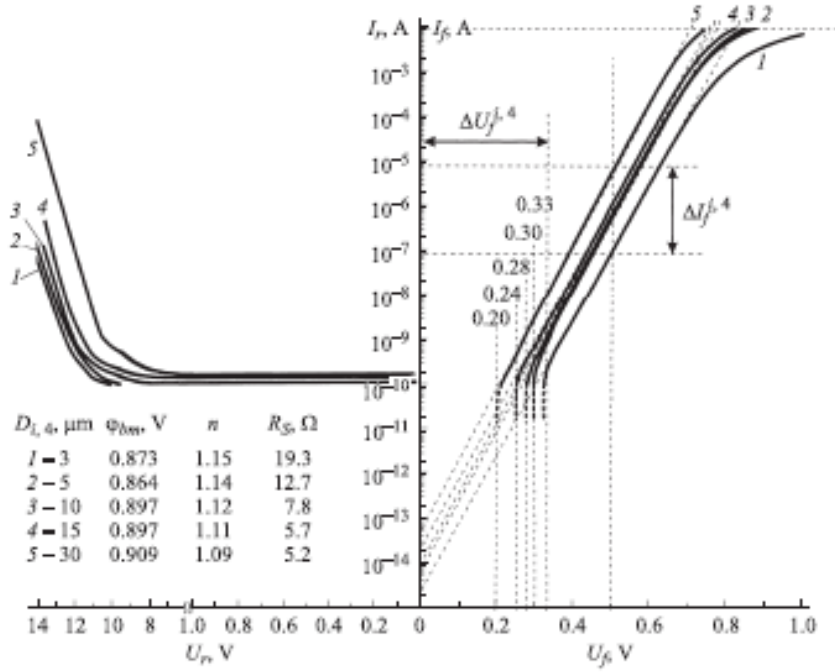

Figure 16. Forward and reverse I-V characteristics are not electrically interacting Au-nGaAs Schottky diodes with a diameter $D_{i,4}$: 1 - 3 μm, 2 - 5 μm, 3 - 10 μm, about 4 - 15 μm and 5 - 30 μm belonging matrices $M_{i,4}$ tenfold respective distance $H_{i,4} = 10xD_{i,4}$ between the Schottky diodes.

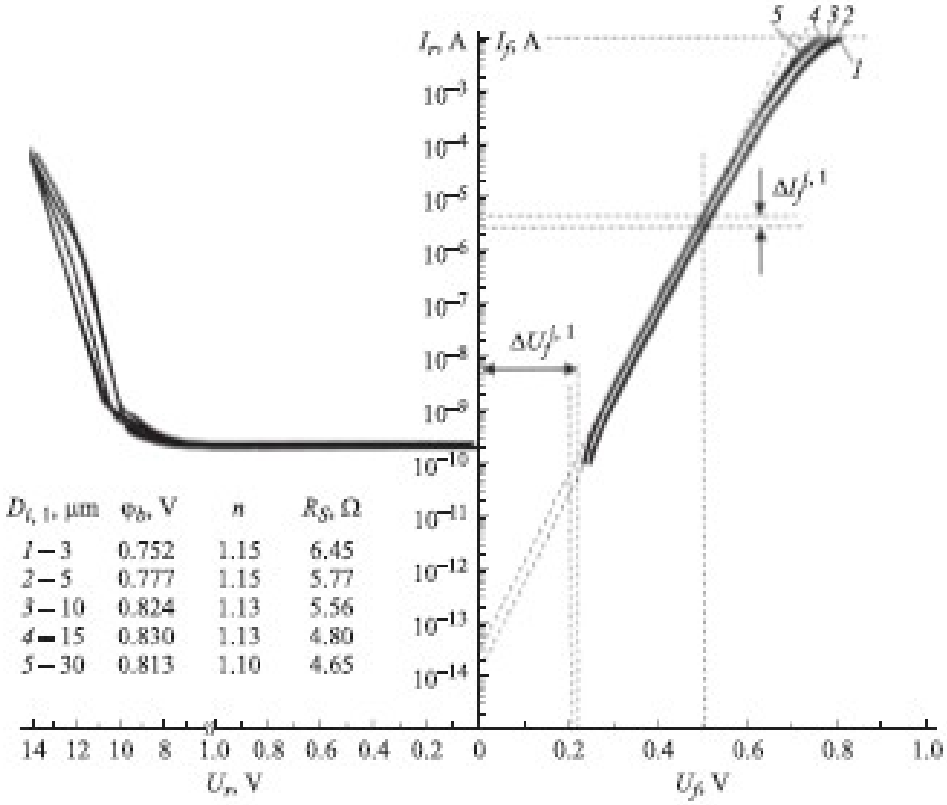

Figure 17. Forward and reverse I-V characteristic electrically interacting Au-nGaAs Schottky diodes with a diameter $D_{i,1}$: 1- 3 μm, 2- 5 μm, 3 – 10 μm, 4 – 15 μm and 5 – 30 μm, belonging matrices $M_{i,1}$ single respective distance $H_{i,1}=10xD_{i,1}$ between the Schottky diodes.

Features of photoconductivity Schottky diodes with AEF depending on the configuration of contacts

Conversion of light energy into electrical energy occurs in the space charge region (SCR) of the Schottky diode as a result of absorption of photons and the generation of electron - hole pairs. The separation of charges (electrons and holes) by the electric field in the SCR contact leads to the appearance of photovoltage and the emergence of the generation of the photocurrent. AEF in real SD penetrates and covers peripheral semiconductor contact region SCR for extensive contacts (figure 1b,c) and full near contact area SCR for narrow contacts. In [20] firmly established that under the action of the AEF MSC is a marked change in device characteristics and increase the efficiency of conversion of light energy into electrical energy. In this case, investigated Au-nGaAs SD same area S (where, S = 7853.98 μm^2) and metal thickness of 0.1 μm, but different shapes (figure

18) formed on the surface of the epitaxial layer nGaAs (100) with thickness of 10 μm and a concentration $N_D = 6{,}4.10^{14}$ cm^{-3}.

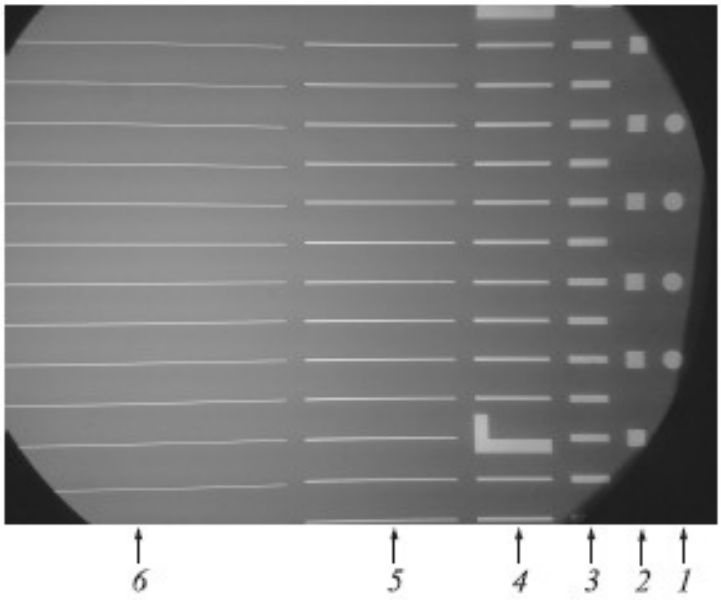

Figure 18. Optical image of Au-nGaAs Schottky diodes same area of S = 7853.98 μm^2 different (i) forms: 1 - round diameter of 100 μm, 2 - square with sides of 88.62 μm^2, 3 - rectangular with sides 40x196.35 μm^2, 4 - rectangular with sides 20x392. 70 μm^2, 5 - rectangular with sides 10x785.40 μm^2, 6 - rectangular with sides 5x1570.80 μm^2.

Figure 19 presents the dark (a) and the corresponding light (b) forward I-V characteristics of Schottky diodes 1 - 6. Seen that saturation currents forward dark I-V characteristics 1-6 have similar values. The I-V characteristics values defined by the existing barrier height diodes 1-6 slightly decrease with increasing perimeter (Table 3).

Table 3

Geometric dimensions of contacts 1- 6 and their dark instrument characteristics

Contacts	**Dimensions of contact (μm)**	**P (μm)**	**I_{of} A**	**Φ_B eV**	**n**	**I_{or} A**	**$J_r = I_{or}/P$ A/μm**
1	D = 100	314,16	$3{\cdot}10^{-13}$	0925	1,05	$3{\cdot}10^{-8}$	$9{,}6.10^{-11}$
2	88,62 x 88,62	354,49	$4{,}3{\cdot}10^{-13}$	0916	1,06	$4{,}5{\cdot}10^{-8}$	$12{,}7.10^{-11}$
3	40 x 196,35	472,70	$5{,}2{\cdot}10^{-13}$	0911	1,06	$5{,}5{\cdot}10^{-8}$	$11{,}6.10^{-11}$
4	20 x 392,70	825,40	$7{,}4{\cdot}10^{-13}$	0902	1,07	$8{\cdot}10^{-8}$	$9{,}7.10^{-11}$
5	10 x 785,4	1590,80	$9{\cdot}10^{-13}$	0897	1,08	$1{,}5{\cdot}10^{-7}$	$9{,}4.10^{-11}$
6	5 x 1570,8	3157,60	$1{\cdot}10^{-12}$	0894	1,09	$2{,}5{\cdot}10^{-7}$	$7{,}9.10^{-11}$

Increase in the length of the perimeter more than 10 times , resulting in an increase in the reverse current in10 times . The linear density of the reverse current of 1-6 contacts at a voltage 10 V has a same value. This means that the reverse currents contacts 1-6 consist only of peripheral currents.

Lighting contacts leads to a slight decrease in forward saturation currents, corresponding increase in the active barrier height Φ_B and decrease in the values ideality factor n (Table 4). For the light forward I-V characteristics increase in the length of the perimeter P, and in contrast to the dark leads to a further increase in the active barrier height Φ_B and reduce in the value ideality factor (Table 4). Increase in the length of the perimeter more than 10 times, leads to an increase photovoltage values more than 1.5 times .

Table 4

Geometric dimensions of contacts 1- 6 and their light instrument characteristics

Contacts	**Dimensions of contact (µm)**	**P (µm)**	**I_{of} A**	**Φ_B eV**	**n**	**I_{or} A**	**$J_r = I_{or}/P$ A/cm**	**U^{ph} V**
1	D = 100	314,16	$2{,}1 \cdot 10^{-13}$	0,934	1,0	$7 \cdot 10^{-8}$	$2{,}2.10^{-10}$	0,24
2	88,62 x 88,62	354,49	$1{,}8 \cdot 10^{-13}$	0,939	1,0	$4{,}55 \cdot 10^{-7}$	$1{,}3.10^{-9}$	0,28
3	40 x 196,35	472,70	$1{,}5 \cdot 10^{-13}$	0,943	1,0	$9{,}945 \cdot 10^{-7}$	$2{,}1.10^{-9}$	0,31
4	20 x 392,70	825,40	$1 \cdot 10^{-13}$	0,953	1,0	$1{,}42 \cdot 10^{-6}$	$1{,}7.10^{-9}$	0,31
5	10 x 785,4	1590,80	$9 \cdot 10^{-14}$	0,856	1,0	$2{,}85 \cdot 10^{-6}$	$1{,}8.10^{-9}$	0,37
6	5 x 1570,8	3157,60	$8 \cdot 10^{-14}$	0,860	1,0	$4{,}75 \cdot 10^{-6}$	$1{,}5.10^{-9}$	0,38

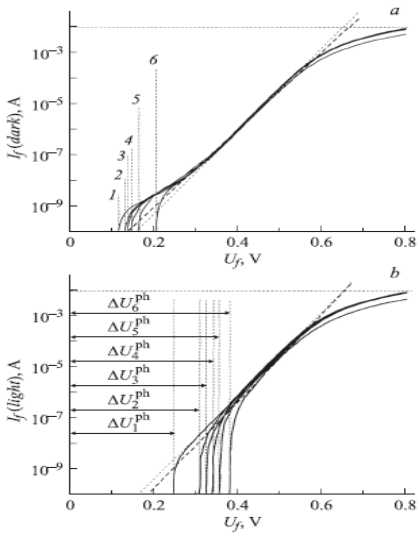

Figure 19. Forward I-V characteristic Au-nGaAs Schottky diodes same area of S = 7853.98 μm^2 different (i) forms (see figure 19): a -the dark and b - the light.

Presented on figure 20 reverse dark (a) and the corresponding light (b) I-V characteristics of Schottky diodes 1-6. As for the dark I-V characteristic, the value of the reverse saturation current the reverse light I-V characteristics increases with the periphery. The values of 2-3 orders of magnitude higher than the values of reverse saturation currents of the dark reverse I-V characteristics indicating a significant reduction in the active barrier height defined by the I-V characteristics. From Table 2 it is seen that by increasing the perimeter of nearly 10 times the photocurrent increases by two orders of magnitude.

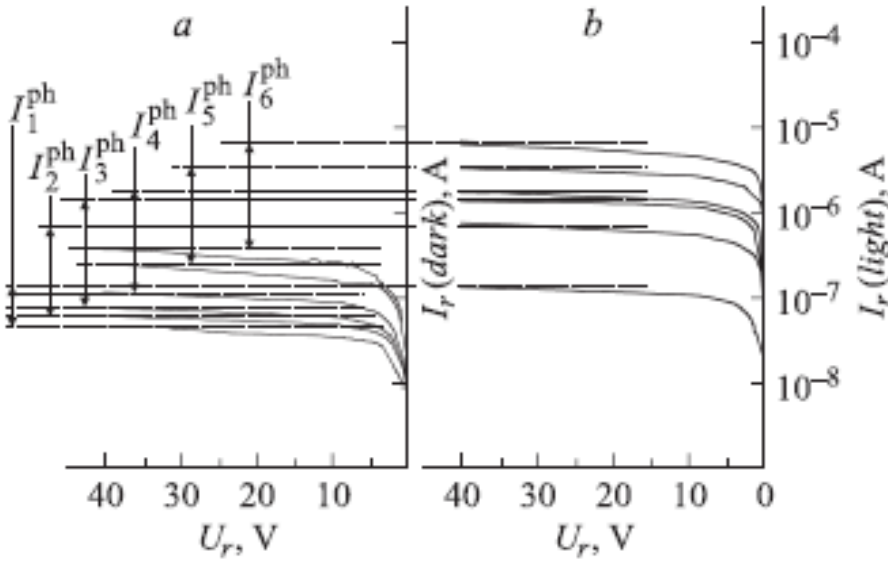

Figure 20. Reverse I-V characteristic Au-nGaAs Schottky diodes same area of S = 7853.98 μm^2 different (i) forms: a - the dark and b - the light.

Thus, to study SD with large perimeter, i.e. significant impact AEF, change device characteristics and efficiency of conversion of light energy into electrical energy is much greater.

Samples MSC diodes with new properties and laws based on AEF

On the basis of the AEF in real MSC already developed semiconductor devices with new properties and regularity. In [20] as a result of extensive AFM studies of MSC with AEF based on Au - nGaAs structures was developed by the MSC to transform the light energy into electrical energy , where the light current exceeds the dark current of more than 1000 times . Meanwhile, in the same MSC converter without AEF photovoltage exceeds the dark current total of about 10 times . Typical light and dark I-V characteristics such performers with high efficiency of conversion of light energy into electrical energy are shown in figure 21. The light I-V characteristics measured at contacts illumination red light with a wavelength equal to 645 nm.

In [21] a study of the current transport and the formation of a potential barrier in the single and matrix narrow MSC with AEF and the contact surface length of 200 μm and widths of 1 μm and 4 μm , fabricated from metal contact Au and n-type semiconductor GaAs with a resistivity 1 Ohm cm was found that the singularity of current transport in narrow SD are in good agreement with the mechanism of thermionic emission current transport in high-quality flat SD in the forward bias and are substantially different in the reverse bias.

Forward I-V characteristics narrow SD represented by straight lines on a semi-logarithmic scale in a wide range of current of about 9 in a row when the voltage increases to 0.7 V and has ideality factor close to unity (figure 22 a). Reverse I-V characteristics narrow SD have specifics unlike I-V characteristics flat SD (figure 22b). Current in narrow SD absent in the initial reverse voltages and further increase in the voltage the current first increases abruptly at voltages of 3-4 V, and then when the voltage increases to about 7V the current increases linearly on the order of 3-5 in semi-logarithmic scale. Saturation currents in the forward and reverse bias coincide. The dependence of the potential barrier height SD on the applied voltage in both directions becomes linear.

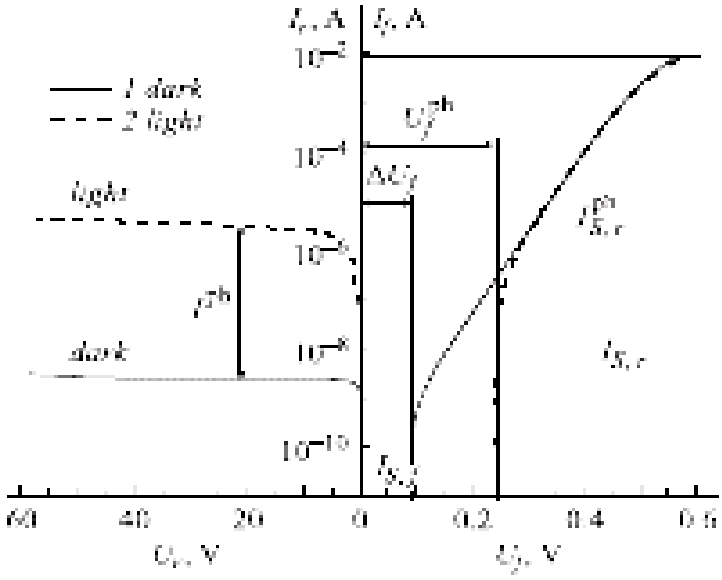

Figure 21. The dark and light forward and reverse current-voltage characteristics of Au-nGaAs converter with an area of 7853.98 μm^2 with AEF and the increased conversion efficiency of light energy into electrical energy.

ward and reverse I-V characteristics and identified organic correlation between the electrophysical parameters .

Energy diagrams of narrow SD were built in the absence of an applied voltage and the presence of the forward and reverse voltage. Found that electronic processes in narrow Au-nGaAs SD well described energy model real contacts metal - semiconductor with AEF [6].

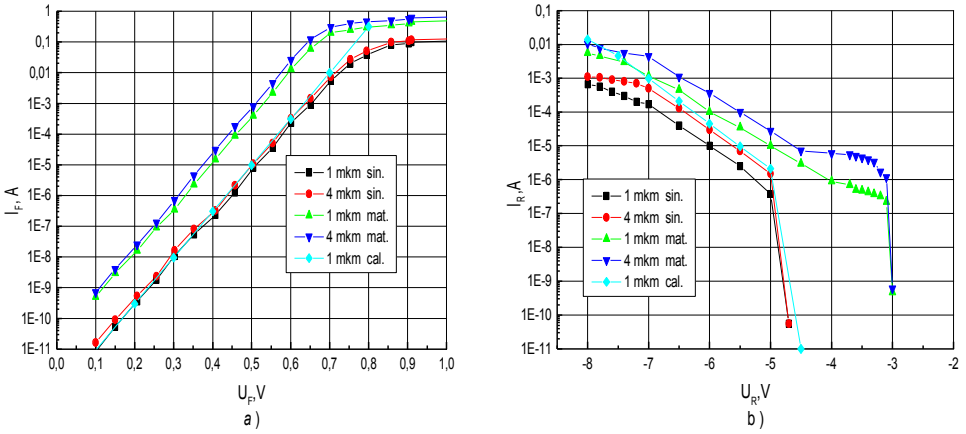

Figure 22. Forward (a) and reverse (b) I-V characteristics of narrow (1 μm and 4 μm) single and matrix Au-nGaAs Schottky diodes with AEF.

Principal structure of semiconductor converters based on NANO - MSC with AEF

Semiconductor converters (SC) on the basis of the MSC are widely used in modern electronic devices to convert various forms of energy into electrical energy. Such SC MSC on the one hand as solar cells, tenzoelement, stress sensors, radioactive emission sensors and others sensors have found extensive use, on the other - their electrical properties are still systematically investigated. Since the electrical processes occurring in such real SC is often difficult to interpret using the main provisions of the fundamental theories and idealized energy models of MSC .

The results of the present experimental and theoretical studies of the firmly established a significant difference in the electrophysical processes occurring in the real and ideal MSC [6,22] . One major reason for this difference is the formation of the MSC due to the AEF as emission heterogeneity in contact interface of materials and in limited contact surface with the free surfaces of the metal and semiconductor. Must be noted that the energy models and mechanisms of current flow in the real MSC considering objectively existing AEF is well enough to explain almost all of the experimentally observed features of electrophysical parameters and characteristics of SC MSC made at various contact structures under various experimental conditions [6].

Semiconductor converters are usually made on the basis of the known theoretical principles implemented on multiple physical elements: p-n junction, heterojunction , the MSC , the metal - insulator - semiconductor structure and metal - insulator - metal structure. Unlike other physical elements, the formation AEF in semiconductor active regions of the near contact real MSC offers the prospect of fabrication of semiconductor MSC based on new physical principles. Since AEF plays an active role in the formation of a potential barrier in

the real MSC and in particular the current flow. In this case the potential barrier MSC is formed even in the case when certain conditions Schottky for rectification MSC had not fulfilled. This is clearly expressed when using metallic and semiconducting nanoparticles as contacting materials for fabrication of semiconductor SC MSC [23].

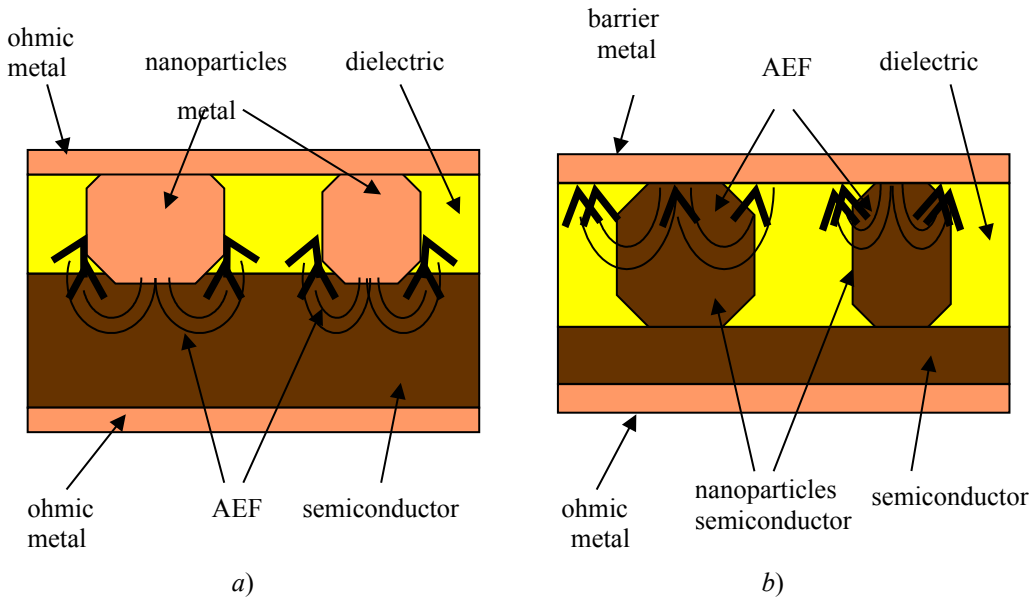

Figure 23. The principal structure of the nano - MSC with AEF semiconductor converters based on metal (a) and semiconductor (b) nanoparticles.

For definiteness, the SC MSC created on the basis of composite materials containing metal and semiconductor nanoparticles in dielectric matrices.

Schematic representation of the SC MSC on the basis of the contact metal nanoparticles in a dielectric matrix with a solid semiconductor plate is presented in figure 23*a*. A certain homogeneous surface of the semiconductor plate with a work function Φ_{BO} applied thin (thickness of the order of the linear dimensions of the nanoparticles) composite film with metallic nanoparticles with a work function Φ_M. At the interfaces of metal nanoparticles and semiconductor plate formed the AEF and the potential barrier height of Φ_{BO} because the contact potential difference between the contact surface with $\Phi_{BO} = \Phi_M - \Phi_S$ and free surfaces of metal Φ_M and semiconductor Φ_S. The structure is provided with ohmic contacts in the form of metal films.

Schematic representation of the SC MSC on the basis of contact semiconductor nanoparticles in a dielectric matrix with a solid metallic plate shown in figure 23b. On the surface of certain metal plate with a work function of Φ_M is applied thin (thickness of the order of the linear dimensions of the nanoparticles) composite film with semiconductor nanoparticles with a work function of Φ_S. At the interfaces of semiconductor nanoparticles and metallic film formed AEF and the potential barrier height of Φ_{BO} due to the contact potential difference between the contact surfaces with $\Phi_{BO} = \Phi_M - \Phi_S$ and free surfaces of the metal and semiconductor Φ_M and Φ_S. The structure is provided with ohmic metal contacts .

Conclusion

Discovery the physical phenomenon of AEF in real MSC there is large event in the modern electronics field, especially in the microelectronics and nanotechnology. It has a fundamental physical basis and firmly confirmed by direct AFM measurements and reliable electrophysical, thermoelectric, photovoltaic and constructive-technological experimental methods.

This phenomenon allows you to open new scientific directions in the areas of semiconductors and semiconductor devices, solid-state, thin films, surfaces, nanophysics, microelectronics, photonics, bioelectronics, nano-electronics, etc. It allows for more depth and detail to interpret the processes occurring in the real contact structures of condensed matter.

The MSC structure is a basic physical element practically all kinds of discrete semiconductor devices and components of integrated micro- and nanocircuits. The AEF phenomenon is the basis of scientific to improve the quality and extend the functionality of the numerous possibilities of discrete semiconductor devices, micro- and nanocircuits, as well as the development of new classes of devices based on the MSC structures.

This phenomenon opens wide prospects for use AFM, SEM and other modern methods for the development and mass production of innovative discrete semiconductor devices, micro- and nanocircuits.

References

[1] Mamedov R. K. The two-barrier physical model of the real metal - semiconductor contacts. Bulletin of Baku University: series fiz.mat.sciences, 2 (2001) 84-94

[2] Broun F. Uber die Stromleitung durx Schwefelmetalle. Ann. Phys. Chem., 153(1874) 556-563

[3] Bardeen J. Semiconductor research leading to the point contact transistor. Nobel Lecture, (1956) December 11

[4] Trigg J. Twentieth century physics: the key experiments, Moscow, 1978

[5] Roderick E.H. Contact metal – semiconductor, Moscow, 1982

[6] Mamedov R. K. Metal - semiconductor contacts with electric spots field, Baku, 2003

[7] Torchov N.A. Surface potential of long-range contacts metal - semiconductor Schottky barrier. Dep.v VINITI number 334-D2008 0m 18.04.2008

[8] Torchov N.A. Influence of the periphery of the contact metal - semiconductor Schottky barrier on their electrical properties. Fizika i Texnika Poluprovodnikov, 45(2011) 70-86

[9] Torchov N.A., Bozhkov V.G., Ivonin I.V., Novikov V.A. The investigation of the potential for locally metallized surface nGaAs by Atomic - Force Microscopy. Surface: X-ray, synchrotron and neutron studies,1(2009) 57-66

[10] Novikov V. A. Research of morphology and electronic properties of a surface of films AIIIBV and contacts metal/AIIIBV a method of atomic-force microscopy. The master's thesis author's abstract, Tomsk, 2010

[11] Torkhov N. A. Nature of electric interaction of Schottky contacts. Fizika i Texnika Poluprovodnikov, 45(2011) 1041-1053

[12] Marcus R.B., Haszko S.E., Murarka S.P., Irvin J.C. Scanning Electron Microscope Studies of Premature Breakdown Sites in GaAs IMPATT Testers. **J.** Electrochem. Soc.: Solid-State Science and Technology. 1974. v.121. № 5. p.692-699

[13] Torkhov N. A. Influence of periphery of contacts metal-semiconductor with Schottky barrier on their static volt-current characteristic. Fizika i Texnika Poluprovodnikov, 44 (2010) 615-624

[14] Mamedov R.K. Features of current flow in real diodes Shottki. Applied Physics (Moscow), 4 (2002) 143-151

[15] Mamedov R.K. Temperature dependence of current flow in Schottky diodes. Applied Physics (Moscow), 1 (2003) 133-141

[16] Mamedov R.K. Temperature dependence of current flow in Schottky diodes in the absence of edge effects. Applied Physics. (Moscow),3 (2003) 103-111

[17] Mamedov R.K. Temperature dependence of current flow along the periphery of the contact diodes Shottki. Applied Physics (Moscow), 4 (2003) 125-133
[18] Mamedov R.K. Temperature dependence of current flow in a Schottky diode at high reverse napryazheniyah.Prikladnaya physics. (Moscow), 5 (2003)118-125
[19] Mamedov R.K. Dependence of current flow in a Schottky diode on the impurity concentration semiconductor. Applied Physics (Moscow), 6 (2003) 134-140
[20] Torkhov N. A. Influence fotoedes on current transport in metal-semiconductor contacts with Schottky barrier. Fizika i Texnika Poluprovodnikov, 45 (2011) **9**65-975
[21] Mamedov R.K., Yeganeh M.A. Current Transport and Formation of Energy Structures in Narrow Schottky diodes. J. Microelectronics Reliability. 52 (2012) 418 – 424
[22] Mamedov R.K. Electrical properties of real contacts metal – semiconductor. Abstract of Doctoral Dissertation, Baku, 2004
[23] Mamedov R.K. Semiconductor converters. Moscow, 2009
http://www.nanometer.ru/2009/04/08/preobrazovatel_barer_shottki_diod_shottki_153822.html

REAL METAL – YARIMKEÇİRİCİ KONTAKTLARIN ƏLAVƏ ELEKTRİK SAHƏSİNİN XÜSUSİYYƏTLƏRİ

R. Q. MƏMMƏDOV

XÜLASƏ

Bu icmalda real metal-yarımkeçirici kontaktlarda (MYK) əvvəllər elmə məlum olmayan əlavə elektrik sahəsinin (ƏES) yaranma hadisəsinin fiziki əsasları əks olunmuşdur. Müxtəlif konfiqurasiyalı, həndəsi ölçülü, kontakt materiallı və aralıq məsafəli MYK-larda ƏES-nin Atom Qüvvə Mikroskopu ilə bilavasitə ölçülmüş nəticələri verilmişdir. Makro, mikro və nanoqurluşlu MYK-ların elektrofiziki, termoelektrik, fotoelektrik və konstruktiv-texnoloji eksperimental ölçmələrində ƏES-in xüsusiyyətləri göstərilmişdir.

Açar sözlər: metal-yarımkeçirici kontakt, Şottki diodu, Şottki çəpəri, əlavə elektrik sahəsi, yarımkeçirici çevricilər.

ОСОБЕННОСТИ ДОПОЛНИТЕЛЬНОГО ЭЛЕКТРИЧЕСКОГО ПОЛЯ В РЕАЛЬНЫХ КОНТАКТАХ МЕТАЛЛ – ПОЛУПРОВОДНИК

Р. К. МАМЕДОВ

РЕЗЮМЕ

В данном обзоре изложены физические основы неизвестного ранее физического явления возникновения дополнительного электрического поля (ДЭП) в реальных контактах металл – полупроводник (КМП). Представлены результаты непосредственного измерения ДЭП методами Атомно-Силовой Микроскопии в КМП с различными конфигурациями, геометрическими размерами,

контактирующими материалами и расстояниями между ближе расположенных контактов. Показаны специфические особенности ДЭП в электрофизических, термоэлектрических, фото-электрических и конструктивно – технологических экспериментальных измерениях КМП с макро, микро и наноструктурами.

Ключевые слова: контакт металл – полупроводник, диод Шоттки, барьер Шоттки, дополнительное электрическое поле, полупроводниковые преобразователи.

Received: 20.11.2013
Signed for printing: 12.27.2013